

Locally-Verifiable Sufficient Conditions for Exactness of the Hierarchical B-spline Discrete de Rham Complex in \mathbb{R}^n

Shepherd, Kendrick; Toshniwal, Deepesh

DOI

[10.1007/s10208-024-09659-6](https://doi.org/10.1007/s10208-024-09659-6)

Publication date

2024

Document Version

Final published version

Published in

Foundations of Computational Mathematics

Citation (APA)

Shepherd, K., & Toshniwal, D. (2024). Locally-Verifiable Sufficient Conditions for Exactness of the Hierarchical B-spline Discrete de Rham Complex in \mathbb{R}^n . *Foundations of Computational Mathematics*. <https://doi.org/10.1007/s10208-024-09659-6>

Important note

To cite this publication, please use the final published version (if applicable). Please check the document version above.

Copyright

Other than for strictly personal use, it is not permitted to download, forward or distribute the text or part of it, without the consent of the author(s) and/or copyright holder(s), unless the work is under an open content license such as Creative Commons.

Takedown policy

Please contact us and provide details if you believe this document breaches copyrights. We will remove access to the work immediately and investigate your claim.



Locally-Verifiable Sufficient Conditions for Exactness of the Hierarchical B-spline Discrete de Rham Complex in \mathbb{R}^n

Kendrick Shepherd¹ · Deepesh Toshniwal²

Received: 3 September 2022 / Revised: 21 December 2023 / Accepted: 19 January 2024

© The Author(s) 2024

Abstract

Given a domain $\Omega \subset \mathbb{R}^n$, the de Rham complex of differential forms arises naturally in the study of problems in electromagnetism and fluid mechanics defined on Ω , and its discretization helps build stable numerical methods for such problems. For constructing such stable methods, one critical requirement is ensuring that the discrete subcomplex is cohomologically equivalent to the continuous complex. When Ω is a hypercube, we thus require that the discrete subcomplex be exact. Focusing on such Ω , we theoretically analyze the discrete de Rham complex built from hierarchical B-spline differential forms, i.e., the discrete differential forms are smooth splines and support adaptive refinements—these properties are key to enabling accurate and efficient numerical simulations. We provide locally-verifiable sufficient conditions that ensure that the discrete spline complex is exact. Numerical tests are presented to support the theoretical results, and the examples discussed include complexes that satisfy our prescribed conditions as well as those that violate them.

Keywords de Rham complex · Finite element exterior calculus · Hierarchical B-splines · Discrete differential forms

Mathematics Subject Classification 65N30 · 58J10 · 58A12 · 65D07

Communicated by Doug Arnold.

- ✉ Kendrick Shepherd
kendrick_shepherd@byu.edu
- ✉ Deepesh Toshniwal
d.toshniwal@tudelft.nl

¹ Department of Civil and Construction Engineering, Brigham Young University, Provo, UT 84602, USA

² Delft Institute of Applied Mathematics, Delft University of Technology, Delft, The Netherlands

1 Introduction

While many partial differential equations (PDEs) may be couched as minimization problems, a large swath of them are more naturally described as saddle-point problems. Numerical solutions of these PDEs require special care since the discrete problem is not guaranteed to be well-posed for all choices of finite dimensional spaces even if the continuous problem is. For instance, it may be necessary to verify (for each combination of finite dimensional spaces) the Ladyzhenskaya–Babuska–Brezzi condition for problems of interest such as electromagnetism and fluid flows. On the other hand, the language of exterior calculus provides an abstract framework that can be used to uniformly discuss a large class of PDEs as well as their discretizations. This framework has yielded an elegant approach, dubbed *finite element exterior calculus* [2, 3], for developing well-posed discrete formulations. In this document, and for problems posed on n -dimensional domains in \mathbb{R}^n , $n \geq 1$, we provide new theoretical results that can help build such well-posed discretizations using finite dimensional spaces of locally-refinable spline functions.

The use of spline functions for numerically solving PDEs has been popularized by the emergence of *isogeometric analysis* [16]. A generalization of the classical finite element method [17], the isogeometric analysis philosophy relies on the use of spline functions [9, 23] for describing both the domain on which the problem is posed as well as the discrete solution. One objective of this approach is to greatly simplify the application of numerical methods to geometries of engineering interest, which are themselves designed within computer-aided design software using spline functions [13]. The last two decades have seen this approach applied successfully to challenging problems such as full scale wind turbine simulations [4] and performance assessment of cardiac implants [19]. Moreover, recent theoretical developments [5, 22] have also given credence to the large amounts of numerical evidence that suggested that smooth splines demonstrate better approximation behaviour per degree of freedom than less smooth or classical C^0 and C^{-1} finite element spaces [10].

Therefore, in this document we focus on methods that extend finite element exterior calculus by utilizing smooth splines in lieu of the classical C^0 and C^{-1} finite element spaces. The existing approaches [6, 7, 11] in this line of research have predominantly focused on PDEs that arise as Laplacians of the de Rham cochain complex of (L^2 completions of) smooth differential forms. The said approaches either focus on identifying spline spaces that can be used to stably discretize such PDEs [6, 8, 12, 18, 26], or they use those spline spaces in applications of interest such as magnetohydrodynamics [21], where exact satisfaction of physical conservation laws in the discrete setting is desirable.

When identifying stable discretizations for a PDE arising from some cochain complex, one of the main considerations in (spline-based) finite element exterior calculus is the identification of discrete spaces that together form a cohomologically-equivalent subcomplex of the continuous one.¹ Evans et al. [12] were the first to study this for locally refinable spline functions called hierarchical B-splines [20]. Their main result identifies sufficient conditions for ensuring that the hierarchical B-spline spaces on a

¹ The other main considerations (e.g., commuting projections) are outside the scope of the present work.

rectangular $\Omega \subset \mathbb{R}^2$ form an exact subcomplex of the de Rham complex of L^2 differential forms on Ω . In this manuscript, we generalize and extend this to subdomains of \mathbb{R}^n for any $n \geq 1$. The main contribution of this manuscript is the identification of locally-verifiable sufficient conditions that guarantee the exactness of the complex of hierarchical B-spline differential forms defined on a box (a.k.a. a hypercube) $\Omega \subset \mathbb{R}^n$.

We describe our main result here (albeit a bit imprecisely) so that a reader familiar with hierarchical B-splines [20] and the complex of B-spline differential forms [6] can get a flavor of our main result.

Theorem Consider an n -dimensional box $\Omega \subset \mathbb{R}^n$ and an associated domain hierarchy

$$\Omega =: \Omega_0 \supseteq \Omega_1 \supseteq \dots \supseteq \Omega_L \supseteq \Omega_{L+1} := \emptyset .$$

On each Ω_ℓ , define a complex of tensor-product B-spline differential forms as in [6] and, assuming nestedness, use Kraft’s selection mechanism [20] to build a complex of hierarchical B-spline differential forms [12]. Moreover, assume the following for any $\ell < L$.

- $\Omega_{\ell+1}$ is the union of supports of level ℓ B-spline 0-forms.
- If a level- ℓ or level- $(\ell + 1)$ B-spline, ϕ , is supported on a union A of refined level- ℓ 0-form B-splines, then there is a “nearby” level- ℓ 0-form B-spline α such that $\text{supp}(\phi) \subset \text{supp}(\alpha) \subset \Omega_{\ell+1}$.
- If two level ℓ B-spline 0-forms α_i and α_j are supported on $\Omega_{\ell+1}$, and if the intersections of their supports has a “minimal size”, then there exists a “shortest chain” of level ℓ B-spline 0-forms from α_i to α_j , with each B-spline in the chain supported on $\Omega_{\ell+1}$.

Then, the complex of hierarchical B-spline differential forms is exact.

Here, Kraft’s selection mechanism is the selection mechanism of Definition 3.1.

See Definitions 4.1, 4.2, 4.3 and Assumption 3 for the precise statement. Proof of this result is given in Theorem 4.23.

In the above, by a “chain” of B-splines from α_i to α_j , we mean a sequence of B-splines—with the first and the last B-splines in the sequence being α_i and α_j —such that each B-spline in the sequence is obtained from the preceding one by a unit translation of its support in index space [16]. By a “shortest chain”, we mean a sequence with the smallest number of B-splines. Note that this assumption is locally-verifiable, i.e., it can be checked in a local manner for any given hierarchical B-spline mesh.

We start this manuscript by recalling the basics of the de Rham complex of differential forms (Sect. 2) and the construction of the hierarchical B-spline complex (Sect. 3). Section 4 contains our main result, which is derived by using the notion of Mayer–Vietoris sequences [15]. We discuss implementational aspects and present numerical tests that complement our theoretical results in Sect. 5 before concluding in Sect. 6.

2 The de Rham Complex of Differential Forms

Before discussing exactness of the discrete (spline) complex of interest for numerical analysis, we first briefly introduce the continuous de Rham complex that we aim to approximate using these splines. For the sake of clarity and brevity, we do not attempt to fully characterize all of the mathematical objects with which we work. Instead, we emphasize only those properties that will be necessary for understanding the following mathematical presentation. A reader more interested in a full picture may want to read [1] or [24] for a more thorough introduction.

Let $\Omega \subset \mathbb{R}^n$ be a bounded domain with a piecewise-smooth Lipschitz boundary and let $T_{\mathbf{y}}\Omega = \mathbb{R}^n$ denote the n -dimensional tangent space at $\mathbf{y} \in \Omega$. A smooth differential j -form f , $j = 0, \dots, n$, on Ω is a smooth field such that $f_{\mathbf{y}}$ is a real-valued skew-symmetric j -linear form on $T_{\mathbf{y}}\Omega \times \dots \times T_{\mathbf{y}}\Omega$. Let $\Lambda^j(\Omega)$ denote the space of all smooth differential j -forms, $j = 0, \dots, n$.

For $j = 0, \dots, n$, and $f \in \Lambda^j(\Omega)$, the exterior derivative is a linear map, $d^j : \Lambda^j(\Omega) \rightarrow \Lambda^{j+1}(\Omega)$, such that $d^{j+1} \circ d^j = 0$. By convention, d^j is the zero map if $j < 0$ or $j \geq n$, and $\Lambda^j(\Omega) := 0$ if $j < 0$ or $j > n$. For our purposes, we will not need the explicit definition of d^j , only its properties will be sufficient.

With $L^2\Lambda^j(\Omega)$ denoting the completion of $\Lambda^j(\Omega)$ with respect to the L^2 inner product of j -forms $(\cdot, \cdot)_{L^2\Lambda^j(\Omega)}$, we define $H\Lambda^j(\Omega)$ as

$$H\Lambda^j(\Omega) := \left\{ f \in L^2\Lambda^j(\Omega) : d^j f \in L^2\Lambda^{j+1}(\Omega) \right\}. \tag{1}$$

With $(\cdot, \cdot) := (\cdot, \cdot)_{L^2\Lambda^j(\Omega)}$, we equip $H\Lambda^j(\Omega)$ with the following graph norm-induced inner-product,

$$(f, g)_{H\Lambda^j(\Omega)} := (f, g) + (d^j f, d^j g). \tag{2}$$

Note that $H\Lambda^0 = H^1(\Omega)$ and $H\Lambda^n(\Omega) = L^2(\Omega)$. Then, the L^2 de Rham complex on Ω is the bounded (since all d^j are bounded linear operators) and closed (since image each d^j is closed in $H\Lambda^{j+1}$) Hilbert complex defined as

$$\mathcal{R} : H\Lambda^0(\Omega) \xrightarrow{d^0} H\Lambda^1(\Omega) \xrightarrow{d^1} \dots \xrightarrow{d^{n-1}} H\Lambda^n(\Omega). \tag{3}$$

The composition property of the exterior derivative implies that the following containment holds for all j ,

$$\text{Im}(d^{j-1}) \subseteq \text{Ker}(d^j). \tag{4}$$

Members of $H\Lambda^j$ in $\text{Ker}(d^j)$ are called j -cocycles or closed, and the members of $H\Lambda^j$ in $\text{Im}(d^{j-1})$ are called j -coboundaries or exact. The j^{th} cohomology space associated to the complex \mathcal{R} , $H^{(j)}(\mathcal{R})$, is defined as the following quotient,

$$H^{(j)}(\mathcal{R}) = \text{Ker}(d^j) / \text{Im}(d^{j-1}). \tag{5}$$

The cohomology space $H^{(j)}(\mathcal{R})$ measures the extent to which the equality in Eq. (4) fails to hold. When Ω is contractible, we have $H^{(0)}(\mathcal{R}) = \mathbb{R}$ and $H^{(j)}(\mathcal{R}) = 0$, $j = 1, \dots, n$.

In this document, we will only consider the variant of \mathcal{R} with homogeneous boundary conditions. This complex is built up from spaces with vanishing boundary conditions,

$$\mathcal{R}_0 : H\Lambda_0^0(\Omega) \xrightarrow{d^0} H\Lambda_0^1(\Omega) \xrightarrow{d^1} \dots \xrightarrow{d^{n-1}} H\Lambda_0^n(\Omega), \tag{6}$$

where $H\Lambda_0^j(\Omega)$ is the space of j -forms with vanishing trace on $\partial\Omega$, $j = 0, \dots, n - 1$, and $H\Lambda_0^n(\Omega) = H\Lambda^n(\Omega)$; see [1] for details. When Ω is contractible, we have $H^{(j)}(\mathcal{R}_0) = 0$, $j = 0, \dots, n - 1$ and $H^{(n)}(\mathcal{R}_0) = \mathbb{R}$.

Finally, we would like to briefly recall the notion of cochain maps. Let $\mathcal{V} = (V, d_V)$ and $\mathcal{W} = (W, d_W)$ be two subcomplexes of \mathcal{R}_0 , i.e., for all j , $V_j, W_j \subseteq H\Lambda_0^j$ and d_V^j and d_W^j are obtained by restrictions of the exterior derivative d^j . Then, linear maps $f^j : V^j \rightarrow W^j$ are called cochain maps if they commute with the differentials for all j ,

$$d_W^j \circ f^j = f^{j+1} \circ d_V^j. \tag{7}$$

Cochain maps preserve closed and exact forms and, consequently, induce maps between cohomology spaces of the two complexes, $f^{*(j)} : H^{(j)}(\mathcal{V}) \rightarrow H^{(j)}(\mathcal{W})$. Additionally, if \mathcal{W} is a subcomplex of \mathcal{V} , the inclusion $\iota : \mathcal{W} \rightarrow \mathcal{V}$ is a cochain map and induces a natural map between their cohomologies. If, additionally, there exists a cochain projection map from \mathcal{V} to \mathcal{W} , it induces a surjection of cohomologies. In particular, the dimensions of $H^{(j)}(\mathcal{W})$ are then bounded from above by those of $H^{(j)}(\mathcal{V})$ for all j .

3 Notation and Preliminaries

We now set the framework to define the hierarchical B-spline complex of discrete differential forms, proceeding largely as in [12], albeit in parametric dimension n . We begin by describing the univariate scenario. Note that all the spaces defined here already incorporate the relevant homogeneous boundary conditions.

3.1 Univariate B-splines

Given polynomial degree $p \geq 1$ and an integer $m \geq 1$, consider a knot vector, i.e., a non-decreasing sequence of real numbers called knots, $\Xi = (\xi_1, \dots, \xi_{m+p+1})$, such that

$$\xi_1 = \dots = \xi_p < \xi_{p+1} \leq \dots \leq \xi_{m+1} < \xi_{m+2} = \dots = \xi_{m+p+1}. \tag{8}$$

For simplicity, we will assume that all knot vectors are such that $\xi_1 = 0, \xi_{m+p+1} = 1$. Note that the first and last knots both appear with multiplicity p . We also assume that no other knot in Ξ appears more than p times.

Given knot vector Ξ , we will define two spaces of piecewise-polynomial functions. First, denote with $\mathcal{X}^0(\Xi)$ the space of piecewise-polynomial functions of degree p defined on the partition of $[0, 1]$ defined by the unique values of the knots ξ_i , such that:

- the functions are C^{p-r} smooth at a knot ξ_i that appears in Ξ with multiplicity r , and,
- the functions vanish at $\xi = 0$ and $\xi = 1$.

Next, denote with $\mathcal{X}^1(\Xi)$ the space of piecewise-polynomial functions of degree $p - 1$ defined on the partition of $[0, 1]$ defined by the unique values of the knots ξ_i , such that the functions are C^{p-r-1} smooth at a knot ξ_i that appears in Ξ with multiplicity r .

The dimension of $\mathcal{X}^j(\Xi)$ is $m + j, j = 0, 1$, and we can define $m + j$ basis functions that span $\mathcal{X}^j(\Xi)$. We will choose univariate B-splines as the basis for these spaces and we will denote them with $\phi_{i,p}^j, i = 1, \dots, m + j$; the set containing these basis functions will be denoted as $\mathcal{B}^j(\Xi)$. This basis has many useful properties, and the ones most interesting for this manuscript are the boundary conditions satisfied by the functions (by definition) and minimal support.

- Boundary conditions: All B-splines $\phi_{i,p}^0$ vanish at positions $\xi = 0$ and $\xi = 1$. Moreover, the only B-splines $\phi_{i,p}^1$ that are non-zero at $\xi = 0$ and $\xi = 1$ are, respectively, $\phi_{1,p}^1$ and $\phi_{m+1,p}^1$.
- Minimal support: We will need the fact that $\text{supp}(\phi_{i,p}^j) = (\xi_i, \xi_{i+p-j+1})$ and, moreover, $\phi_{i,p}^j$ is defined by, and thus can be uniquely identified with, the following subsequence of Ξ ,

$$\phi_{i,p}^j \longleftrightarrow \Xi[i]^j := (\xi_i, \dots, \xi_{i+p-j+1}). \tag{9}$$

By convention, we will define all supports to be open sets in this manuscript. Hereafter, we will exclusively employ this unique identification, i.e., instead of talking about $\phi_{i,p}^j$, we will only talk about $\Xi[i]^j$.

The last things we define in the univariate setting are the Bézier and Greville meshes. The knots in Ξ partition $(0, 1)$ into a mesh that will be called the univariate Bézier mesh and denoted as $M(\Xi)$. Moreover, we associate the B-spline $\Xi[i]^0$ with a point in $(0, 1)$ called the i th Greville point² which is defined as

$$\mu(\Xi[i]^0) := \frac{\xi_{i+1} + \dots + \xi_{i+p}}{p}, \quad i = 1, \dots, m, \tag{10}$$

² Ignore boundary conditions and consider degree p B-splines defined on the augmented knot vector $(\xi_0, \Xi, \xi_{m+p+2})$, with $\xi_0 = 0$ and $\xi_{m+p+2} = 1$. Then, the linear polynomial $f(\xi) = \xi$ can be expressed as a unique linear combination of the B-splines $\Xi[i]^0, i = 0, \dots, m + 1$ and the points $\mu(\Xi[i]^0), i = 0, \dots, m + 1$, are the corresponding coefficients of linear combination.

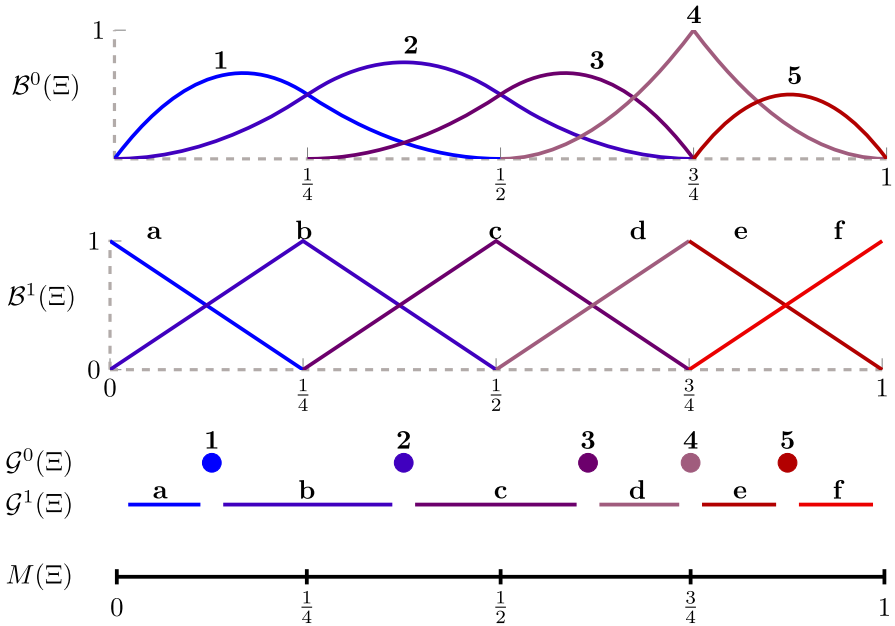


Fig. 1 The one-to-one correspondence between a set of univariate splines with a Greville grid is shown here in one dimension. On the top, the quadratic B-spline basis $\mathcal{B}^0(\Xi)$ corresponding to $\Xi = \{0, 0, \frac{1}{4}, \frac{1}{2}, \frac{3}{4}, \frac{3}{4}, 1, 1\}$ is shown. Below this, the spline basis $\mathcal{B}^1(\Xi)$ is shown. The Greville points $\mathcal{G}^0(\Xi)$ and edges $\mathcal{G}^1(\Xi)$ are shown next. Basis functions of $\mathcal{B}^0(\Xi)$ are in one-to-one correspondence with points of $\mathcal{G}^0(\Xi)$ as indicated with the numerical labeling, while basis functions of $\mathcal{B}^1(\Xi)$ are in one-to-one-correspondence with edges of $\mathcal{G}^1(\Xi)$ through the alphabetically labeled relationship. Finally, the univariate Bézier mesh, $M(\Xi)$, is shown at the bottom, with ticks indicating vertices

and introduce the convention that $\mu(\Xi[0]^0) := 0$ and $\mu(\Xi[m + 1]^0) = 1$. By the assumptions placed on the knots, $0 = \mu(\Xi[0]^0) < \mu(\Xi[1]^0) < \dots < \mu(\Xi[m]^0) < \mu(\Xi[m + 1]^0) = 1$. The Greville points help partition $[0, 1]$ into $(m + 1)$ intervals. We will call the interior of the i th interval in this partition a Greville edge identified with the B-spline $\Xi[i]^1$,

$$\mu(\Xi[i]^1) := (\mu(\Xi[i - 1]^0), \mu(\Xi[i]^0)), \quad i = 1, \dots, m + 1. \tag{11}$$

Then, collecting the Greville points in the set $\mathcal{G}^0(\Xi)$ and the Greville edges in the set $\mathcal{G}^1(\Xi)$, the mesh and formed by them will be called a Greville mesh and will be denoted by $\mathcal{G}(\Xi)$. Finally, $g^j(\Xi)$ will denote the map that performs the above identification of B-splines with the j -dimensional Greville mesh entities,

$$g^j(\Xi) : \mathcal{B}^j(\Xi) \rightarrow \mathcal{G}^j(\Xi). \tag{12}$$

Figure 1 shows an example of the B-splines in $\mathcal{B}^j(\Xi)$ and their correspondence to the members of $\mathcal{G}^j(\Xi)$. Note that the evaluation of the B-spline basis functions can be performed, for instance, with the Cox–de Boor recursion formula [9].

3.2 Tensor-Product B-splines

Using the univariate splines defined above, tensor products can be used to define multivariate spline spaces and a basis for them. Specifically, on $\Omega = (0, 1)^n \subset \mathbb{R}^n$, a tensor product spline space and its B-spline basis are defined by choosing n univariate knot vectors and taking the tensor-products of the associated univariate spline spaces and their B-spline bases, respectively.

With a view toward the next sections where we introduce the hierarchical spline spaces, we describe here the construction of $L + 1$ nested tensor-product spline spaces, $L \geq 0$. Given $0 \leq \ell \leq L$, let the knot vectors in the k th direction be denoted by $\Xi_{\ell,k}$, $k = 1, \dots, n$. We assume that these univariate knot vectors satisfy the assumptions placed on knot vectors in the previous subsection. With $p_{(\ell,k)}$ denoting the corresponding polynomial degree, we will define the spaces $\mathcal{X}^{j_k}(\Xi_{\ell,k})$, $j_k \in \{0, 1\}$ as in the previous subsection, and the dimension of $\mathcal{X}^0(\Xi_{\ell,k})$ will be denoted by $m_{(\ell,k)}$; the dimension of $\mathcal{X}^1(\Xi_{\ell,k})$ will thus be $m_{(\ell,k)} + 1$.

Then, given an n -tuple $\mathbf{j} = (j_1, \dots, j_n)$ such that $j_k \in \{0, 1\}$ for all k , we define the tensor-product spline space $\mathcal{X}_\ell^{\mathbf{j}}$ as the following tensor product of univariate spline spaces,

$$\mathcal{X}_\ell^{\mathbf{j}} := \mathcal{X}^{j_1}(\Xi_{\ell,1}) \otimes \dots \otimes \mathcal{X}^{j_n}(\Xi_{\ell,n}). \tag{13}$$

Remark 3.1 To differentiate notation in the univariate setting from the general tensor-product setting, we will explicitly incorporate the (local) univariate knot vectors in the former; the multidimensional knot vectors will not be included in the latter notation. For instance, we have suppressed the explicit dependence of $\mathcal{X}_\ell^{\mathbf{j}}$ on the underlying knot sequences.

Remark 3.2 Throughout this paper, the multi-index “ \mathbf{j} ” will only appear in superscripts, and all of its entries will take values in $\{0, 1\}$.

Assumption 1 We assume that the knot vectors are nested. That is, for all k and $\ell' > \ell$, if a knot appears in $\Xi_{\ell,k}$ with multiplicity r , then its multiplicity in $\Xi_{\ell',k}$ is at least r . This automatically implies that, for all \mathbf{j} ,

$$\mathcal{X}_0^{\mathbf{j}} \subset \mathcal{X}_1^{\mathbf{j}} \subset \dots \subset \mathcal{X}_L^{\mathbf{j}}. \tag{14}$$

Let us now dive into the details of these spaces and identify the B-splines and the Greville meshes by considering a fixed level $0 \leq \ell \leq L$. The i th knot in $\Xi_{\ell,k}$ will be denoted with $\xi_{i,\ell,k}$. For the k th parametric direction, the i_k th univariate B-spline will be uniquely identified with the local knot vector $\Xi[i_k]_{\ell,k}^{j_k}$. Consequently, the i th tensor-product B-spline $\phi_{\mathbf{i}}^{\mathbf{j}} \in \mathcal{X}_\ell^{\mathbf{j}}$, $1 \leq i_k \leq m_{(\ell,k)} + j_k$ for all k , will be identified with the following Cartesian product of the local knot vectors that define it,

$$\phi_{\mathbf{i}}^{\mathbf{j}} \longleftrightarrow \prod_{k=1}^n \Xi[i_k]_{\ell,k}^{j_k}. \tag{15}$$

All such B-splines in $\mathcal{X}_\ell^{\mathbf{j}}$ will be collected in the set $\mathcal{B}_\ell^{\mathbf{j}}$. Their support is the Cartesian product of the univariate B-splines' support,

$$\text{supp}(\phi_{\mathbf{1}}^{\mathbf{j}}) = \prod_{k=1}^n \text{supp}(\Xi[i_k]_{\ell,k}^{j_k}). \tag{16}$$

The Greville entity in \mathbb{R}^n associated to $\phi_{\mathbf{1}}^{\mathbf{j}}$ is simply the Cartesian product of those associated to the univariate B-splines,

$$\mu(\phi_{\mathbf{1}}^{\mathbf{j}}) = \prod_{k=1}^n \mu(\Xi[i_k]_{\ell,k}^{j_k}). \tag{17}$$

The set \mathcal{G}_ℓ^j will contain all Greville entities $\mu(\phi_{\mathbf{1}}^{\mathbf{j}})$ such that $|\mathbf{j}| = j$, where $|\mathbf{j}| = \sum_{k=1}^n j_k$. The map g_ℓ^j will perform the one-to-one identification of the B-splines with the corresponding elements of \mathcal{G}_ℓ^j ,

$$g_\ell^j : \bigcup_{|\mathbf{j}|=j} \mathcal{B}_\ell^{\mathbf{j}} \rightarrow \mathcal{G}_\ell^j. \tag{18}$$

Combining \mathcal{G}_ℓ^j for all j , we obtain the cuboidal Greville mesh \mathcal{G}_ℓ . Similarly, the tensor-product Bézier mesh M will be defined as the Cartesian product of the univariate meshes defined by the knot vectors $\Xi_{\ell,k}$,

$$M_\ell := \prod_{k=1}^n M(\Xi_{\ell,k}). \tag{19}$$

3.3 Tensor-Product Spline Differential Forms

Using the tensor-product spline spaces $\mathcal{X}_\ell^{\mathbf{j}}$, we can now define the space of tensor-product spline differential j -forms at the ℓ th refinement level as below,

$$\mathcal{X}_\ell^j := \prod_{|\mathbf{j}|=j} \mathcal{X}_\ell^{\mathbf{j}}. \tag{20}$$

Equivalently, we can rewrite the above as follows, noting that all superscripts on the right are n -tuples,

$$\begin{aligned} \text{0-forms, } \mathcal{X}_\ell^0 &:= \mathcal{X}_\ell^{(0,0,\dots,0)}, \\ \text{1-forms, } \mathcal{X}_\ell^1 &:= \mathcal{X}_\ell^{(1,0,\dots,0)} \times \mathcal{X}_\ell^{(0,1,0,\dots,0)} \times \dots \times \mathcal{X}_\ell^{(0,\dots,0,1)}, \\ &\vdots \\ \text{\textit{n}-forms, } \mathcal{X}_\ell^n &:= \mathcal{X}_\ell^{(1,1,\dots,1)}. \end{aligned} \tag{21}$$

As noted in the previous section, j -forms can be naturally identified with j -cells in the Greville mesh.

3.4 Hierarchical B-splines

For all j -forms, $j = 0, \dots, n$, we will use the $(L + 1)$ levels of nested tensor-product spline spaces defined above to build a space of hierarchical B-splines. To do so, we first build a domain hierarchy

$$\Omega =: \Omega_0 \supseteq \Omega_1 \supseteq \dots \supseteq \Omega_L \supseteq \Omega_{L+1} := \emptyset, \tag{22}$$

that helps indicate which tensor-product B-splines contribute to the hierarchical space.

Definition 3.1 (*Hierarchical B-splines*) The set of hierarchical B-splines \mathcal{H}_L^j is constructed using the following recursive algorithm [12, 20, 28]:

1. Initialization, $\ell = 0$: $\mathcal{H}_0^j := \mathcal{B}_0^j$.
2. Recursion, $\ell = 0, \dots, L - 1$: Construct $\mathcal{H}_{\ell+1}^j$ from \mathcal{H}_ℓ^j by setting

$$\mathcal{H}_{\ell+1}^j = \mathcal{H}_{\ell+1,c}^j \cup \mathcal{H}_{\ell+1,f}^j,$$

where

$$\begin{aligned} \mathcal{H}_{\ell+1,c}^j &:= \{ \phi \in \mathcal{H}_\ell^j : \text{supp}(\phi) \not\subset \Omega_{\ell+1} \}, \\ \mathcal{H}_{\ell+1,f}^j &:= \{ \phi \in \mathcal{B}_{\ell+1}^j : \text{supp}(\phi) \subset \Omega_{\ell+1} \}. \end{aligned}$$

For $\ell = 0, \dots, L$, the spaces of hierarchical splines \mathcal{W}_ℓ^j are simply defined to be the span of \mathcal{H}_ℓ^j ,

$$\mathcal{W}_\ell^j := \langle \mathcal{H}_\ell^j \rangle. \tag{23}$$

Taking inspiration from [12, 28], we place the following assumption on these domains. This is a common assumption on the construction of hierarchical spline spaces and places a (level-dependent) lower-bound on the sizes of the refinement domains.

Assumption 2 The subdomain $\Omega_{\ell+1}$ is given as the union of supports of 0-form basis functions from the previous level. That is, for $\ell = 0, \dots, L - 1$, there exists $S \subset \mathcal{B}_\ell^0$ such that

$$\Omega_{\ell+1} = \bigcup_{\alpha \in S} \text{supp}(\alpha). \tag{24}$$

3.5 Hierarchical Spline Differential Forms

Using the above definition, and similarly to the tensor-product case, we define the spaces of hierarchical B-spline differential forms, \mathcal{W}_ℓ^j , $j = 0, \dots, n$, $\ell = 0, \dots, L$, as

$$\mathcal{W}_\ell^j := \prod_{|\mathbf{j}|=j} \mathcal{W}_\ell^{\mathbf{j}}. \tag{25}$$

Equivalently, we can rewrite the above as follows, noting that all superscripts on the right are n -tuples,

$$\begin{aligned} \text{0-forms, } \mathcal{W}_\ell^0 &:= \mathcal{W}_\ell^{(0,0,\dots,0)}, \\ \text{1-forms, } \mathcal{W}_\ell^1 &:= \mathcal{W}_\ell^{(1,0,\dots,0)} \times \mathcal{W}_\ell^{(0,1,0,\dots,0)} \times \dots \times \mathcal{W}_\ell^{(0,\dots,0,1)}, \\ &\vdots \\ \text{\(n\)-forms, } \mathcal{W}_\ell^n &:= \mathcal{W}_\ell^{(1,1,\dots,1)}. \end{aligned} \tag{26}$$

For ease of reading, we will reserve certain symbols for referring to (hierarchical) B-splines and general (hierarchical) splines for certain choices of j ; we tabulate this in Table 1, below. This notation will be reused for the entirety of this document, and is also consistent with the notation used thus far.

4 Exactness of the n -Dimensional Hierarchical Spline Complex of Differential Forms

We now present several results that will be useful for proving exactness of the hierarchical spline de Rham complex in n dimensions. Section 4.1 collects some elementary results from algebraic topology without proof, since their proofs can be found in multiple references; we will use [25] as our main reference. Section 4.2 contains the main result of this paper—a proof of exactness for the n -dimensional hierarchical B-spline complex under suitable assumptions.

Table 1 To simplify reading of the text, the following symbols will be reserved and consistently reused for talking about (B-)spline differential forms

j -forms	(Hierarchical) B-splines	General splines
$j = 0$	α	a
$j = n$	ζ	z
Unspecified j	ϕ	f

Table 2 General and shorthand notation corresponding to Eq. (27) that will be used extensively in the following sections for different choices of $Y \subset \Omega$

Sub-domain	(Shorthand) notation for (27)			
$Y \subset \Omega$	$\mathcal{B}_\ell^j(Y)$	$\mathcal{X}_\ell^j(Y)$	$\mathcal{X}_\ell^j(Y)$	$\mathcal{G}_\ell(Y)$
$Y = \Omega_{\ell'}, \ell' \geq \ell$	$\mathcal{B}_{\ell, \ell'}^j$	$\mathcal{X}_{\ell, \ell'}^j$	$\mathcal{X}_{\ell, \ell'}^j$	$\mathcal{G}_{\ell, \ell'}$
$Y = \Omega$	\mathcal{B}_ℓ^j	\mathcal{X}_ℓ^j	\mathcal{X}_ℓ^j	\mathcal{G}_ℓ

Observe that the notation in the last row above coincides with definitions introduced previously in Sect. 3.2

4.1 Mayer–Vietoris on Spline Functions

We start by defining here some notation and associated shorthand that will be used extensively in the following. The purpose is to collect and highlight the definitions so that the reader can easily find them, as well as compare them against similar notations that will be introduced later in Sect. 4.2. We define a special subset of B-splines in \mathcal{B}_ℓ^j (and the associated spline space, Greville submesh and the space of j -forms), denoted $\mathcal{B}_\ell^j(Y)$, that contains B-splines in \mathcal{B}_ℓ^j that are supported on $Y \subset \Omega$, i.e.,

$$\mathcal{B}_\ell^j(Y) := \left\{ \phi \in \mathcal{B}_\ell^j : \text{supp}(\phi) \subset Y \right\}, \tag{27a}$$

$$\mathcal{X}_\ell^j(Y) := \left\langle \mathcal{B}_\ell^j(Y) \right\rangle, \tag{27b}$$

$$\mathcal{X}_\ell^j(Y) := \bigtimes_{|\mathbf{j}|=j} \mathcal{X}_\ell^j(Y), \tag{27c}$$

$$\mathcal{G}_\ell(Y) := \bigcup_{\substack{\phi \in \mathcal{B}_\ell^j(Y) \\ 0 \leq |\mathbf{j}| \leq n}} g_\ell^{|\mathbf{j}|}(\phi). \tag{27d}$$

This notation and the associated shorthand is collected in Table 2 for convenience. Observe that the last row of Table 2 coincides with definitions introduced previously.

4.1.1 Local Cochain Complexes

For the domain Ω , the coboundary operator for the de Rham cochain complex of differential forms is the exterior derivative, $d^j : H\Lambda_0^j(\Omega) \rightarrow H\Lambda_0^{j+1}(\Omega)$, and it maps j -forms to $(j + 1)$ -forms and enjoys the property

$$d^{j+1} \circ d^j = 0. \tag{28}$$

For any subspace of $H\Lambda_0^j(\Omega)$ (e.g., \mathcal{X}_ℓ^j) the exterior derivative is obtained by restriction of d to the subspace. Note that the combination of the (restrictions of) the exterior derivative with the spaces \mathcal{X}_ℓ^j for $j = 0, \dots, n$, we obtain a cochain complex (\mathcal{X}_ℓ, d)

or simply \mathcal{X}_ℓ ,

$$\mathcal{X}_\ell : \mathcal{X}_\ell^0 \xrightarrow{d^0} \mathcal{X}_\ell^1 \xrightarrow{d^1} \dots \xrightarrow{d^{n-1}} \mathcal{X}_\ell^n. \tag{29}$$

Remark 4.1 For simplicity of notation, and because it will always be clear from the context, we will remove the superscript from the exterior derivative.

By restricting to a subdomain, $Y \subset \Omega$, we can create subcomplexes of the above complex. This is encapsulated in the following elementary results.

Lemma 4.1 For $Y \subset \Omega$, the set of spline spaces $\mathcal{X}_\ell^j(Y)$ for $j = 0, \dots, n$ and (restriction of) exterior derivative define a cochain complex $(\mathcal{X}_\ell(Y), d)$, that is a subcomplex of (\mathcal{X}_ℓ, d) .

Corollary 4.2 Let $X \subset Y \subset \Omega$. Then the cochain complex $(\mathcal{X}_\ell(X), d)$ is a subcomplex of $(\mathcal{X}_\ell(Y), d)$.

With the above definitions in place for the cochain complex $(\mathcal{X}_\ell(Y), d)$, we define the following spaces that respectively contain the ℓ -th level j -forms that are in the kernel and range of the exterior derivative,

$$\text{Ker}_\ell^j(Y) := \left\{ f \in \mathcal{X}_\ell^j(Y) : df = 0 \right\}, \quad \text{Im}_\ell^{j-1}(Y) := \left\{ df : f \in \mathcal{X}_\ell^{j-1}(Y) \right\}. \tag{30}$$

The corresponding j -th cohomology group is then defined as

$$H_\ell^{(j)}(Y) := \text{Ker}_\ell^j(Y) / \text{Im}_\ell^{j-1}(Y). \tag{31}$$

4.1.2 Construction of Mayer–Vietoris Sequences

Let $A, B \subset \Omega$ be domains with cochain complexes $(\mathcal{X}_\ell(A), d)$ and $(\mathcal{X}_\ell(B), d)$. Similarly, define the spline complexes $(\mathcal{X}_\ell(A \cup B), d)$ and $(\mathcal{X}_\ell(A \cap B), d)$. Also, we define

$$\mathcal{B}_\ell^j(A \boxplus B) := \mathcal{B}_\ell^j(A) \cup \mathcal{B}_\ell^j(B), \tag{32a}$$

$$\mathcal{X}_\ell^j(A \boxplus B) := \left\langle \mathcal{B}_\ell^j(A \boxplus B) \right\rangle = \mathcal{X}_\ell^j(A) + \mathcal{X}_\ell^j(B). \tag{32b}$$

Then, we obtain a short exact sequence of chain complexes,

$$\mathcal{X}_\ell(A \cap B) \rightarrow \mathcal{X}_\ell(A) \oplus \mathcal{X}_\ell(B) \rightarrow \mathcal{X}_\ell(A \boxplus B), \tag{33}$$

as shown explicitly in the following commutative diagram.

Lemma 4.3 *The following commutative diagram of short exact sequences holds*

$$\begin{array}{ccccccc}
 & & 0 & & 0 & & 0 \\
 & & \downarrow & & \downarrow & & \downarrow \\
 \dots & \xrightarrow{d} & \mathcal{X}_\ell^{j-1}(A \cap B) & \xrightarrow{d} & \mathcal{X}_\ell^j(A \cap B) & \xrightarrow{d} & \mathcal{X}_\ell^{j+1}(A \cap B) \xrightarrow{d} \dots \\
 & & \downarrow \varphi & & \downarrow \varphi & & \downarrow \varphi \\
 \dots & \xrightarrow{d} & \mathcal{X}_\ell^{j-1}(A) \oplus \mathcal{X}_\ell^{j-1}(B) & \xrightarrow{d} & \mathcal{X}_\ell^j(A) \oplus \mathcal{X}_\ell^j(B) & \xrightarrow{d} & \mathcal{X}_\ell^{j+1}(A) \oplus \mathcal{X}_\ell^{j+1}(B) \xrightarrow{d} \dots \\
 & & \downarrow \psi & & \downarrow \psi & & \downarrow \psi \\
 \dots & \xrightarrow{d} & \mathcal{X}_\ell^{j-1}(A \boxplus B) & \xrightarrow{d} & \mathcal{X}_\ell^j(A \boxplus B) & \xrightarrow{d} & \mathcal{X}_\ell^{j+1}(A \boxplus B) \xrightarrow{d} \dots \\
 & & \downarrow & & \downarrow & & \downarrow \\
 & & 0 & & 0 & & 0
 \end{array}$$

where

$$\varphi : \phi \mapsto (\phi, \phi), \quad \psi : (\phi_1, \phi_2) \mapsto \phi_1 - \phi_2.$$

Moreover, from the above commutative diagram and the Snake Lemma [25, Theorem 2], we obtain a long exact sequence connecting the different cohomologies of the three complexes.

Corollary 4.4 *The following long exact sequence connects the cohomologies and is called the Mayer–Vietoris sequence,*

$$\dots \rightarrow H_\ell^{(j)}(A \cap B) \xrightarrow{\varphi^*} H_\ell^{(j)}(A) \oplus H_\ell^{(j)}(B) \xrightarrow{\psi^*} H_\ell^{(j)}(A \boxplus B) \xrightarrow{\partial^*} H_\ell^{(j+1)}(A \cap B) \rightarrow \dots$$

Due to nestedness of the multi-level spline spaces, the level ℓ spline spaces are contained in the level ℓ' spline spaces, $\ell' \geq \ell$. These inclusions imply the following commutative diagram between the corresponding long exact sequences of cohomologies.

Theorem 4.5 *For domains $A, B \subset \Omega$, $\ell \leq \ell' \leq L$, and the spaces that appear in the Mayer–Vietoris sequence above, the inclusion operator $\iota_{\ell, \ell'} : \mathcal{X}_\ell(\cdot) \rightarrow \mathcal{X}_{\ell'}(\cdot)$ induces a function on cohomology $\iota_{\ell, \ell'}^* : H_\ell^{(j)}(\cdot) \rightarrow H_{\ell'}^{(j)}(\cdot)$ for $j = 0, \dots, n$, such that the following Mayer–Vietoris sequences commute:*

$$\begin{array}{ccccccc}
 \dots & \longrightarrow & H_\ell^{(j)}(A \cap B) & \xrightarrow{\varphi^*} & H_\ell^{(j)}(A) \oplus H_\ell^{(j)}(B) & \xrightarrow{\psi^*} & H_\ell^{(j)}(A \boxplus B) \xrightarrow{\partial^*} H_\ell^{(j+1)}(A \cap B) \longrightarrow \dots \\
 & & \downarrow \iota_{\ell, \ell'}^* & & \downarrow \iota_{\ell, \ell'}^* & & \downarrow \iota_{\ell, \ell'}^* \\
 \dots & \longrightarrow & H_{\ell'}^{(j)}(A \cap B) & \xrightarrow{\varphi^*} & H_{\ell'}^{(j)}(A) \oplus H_{\ell'}^{(j)}(B) & \xrightarrow{\psi^*} & H_{\ell'}^{(j)}(A \boxplus B) \xrightarrow{\partial^*} H_{\ell'}^{(j+1)}(A \cap B) \longrightarrow \dots
 \end{array}$$

Finally, the following result of this section follows from the Five Lemma [15] applied to the commuting diagram from Theorem 4.5.

Corollary 4.6 *Consider the commuting diagram of Mayer–Vietoris sequences from Theorem 4.5. If any two of the following vertical maps are isomorphisms for all j ,*

- $H_\ell^{(j)}(A \cap B) \rightarrow H_{\ell'}^{(j)}(A \cap B)$,
- $H_\ell^{(j)}(A) \oplus H_\ell^{(j)}(B) \rightarrow H_{\ell'}^{(j)}(A) \oplus H_{\ell'}^{(j)}(B)$,
- $H_\ell^{(j)}(A \boxplus B) \rightarrow H_{\ell'}^{(j)}(A \boxplus B)$,

then so is the third map.

4.2 Application of Mayer–Vietoris to Exactness

We are now ready to embark on the exactness proof. The proof has three main steps: decomposition of $\Omega_{\ell+1}$ into small overlapping subdomains; proof that the level ℓ and $\ell + 1$ spline complexes on these subdomains are cohomologically equivalent; and, finally, piecing together the subdomains to show the same for the level ℓ and $\ell + 1$ spline complexes on all of $\Omega_{\ell+1}$. Along the way, we will need to introduce one additional assumption for the third step.

Remark 4.2 All our results are based on the relationship between the refinement domains at two successive levels, and therefore all our figures will only show two levels of refinement.

As in Sect. 4.2, we start by defining some notation and associated shorthand that will be used extensively in what follows. In particular, for $s \in \{0, 1\}$, we define a subset of B-splines in $\mathcal{B}_{\ell+s}^j$ (and the associated spline space, Greville submesh and the space of j -forms), denoted $\mathcal{B}_{\ell+s,\ell+1}^j(Y)$, that contains the B-splines in $\mathcal{B}_{\ell+s}^j$ that are supported on $\text{supp}(\alpha)$ where $\alpha \in \mathcal{B}_{\ell}^0$ is itself supported on $Y \cap \Omega_{\ell+1}$,

$$\mathcal{B}_{\ell+s,\ell+1}^j(Y) := \left\{ \phi \in \mathcal{B}_{\ell+s}^j : \exists \alpha \in \mathcal{B}_{\ell}^0, \text{supp}(\phi) \subset \text{supp}(\alpha) \subset Y \cap \Omega_{\ell+1} \right\}, \tag{34a}$$

$$\mathcal{X}_{\ell+s,\ell+1}^j(Y) := \left(\mathcal{B}_{\ell+s,\ell+1}^j(Y) \right), \tag{34b}$$

$$\mathcal{X}_{\ell+s,\ell+1}^j(Y) := \bigtimes_{|\mathbf{j}|=j} \mathcal{X}_{\ell+s,\ell+1}^{\mathbf{j}}(Y), \tag{34c}$$

$$\mathcal{G}_{\ell}(Y) := \bigcup_{\substack{\phi \in \mathcal{B}_{\ell}^j(Y) \\ 0 \leq |\mathbf{j}| \leq n}} g_{\ell}^{|\mathbf{j}|}(\phi). \tag{34d}$$

This notation and the associated shorthand is collected in Table 3 for convenience. Observe that the shorthand notation in the second row of Table 3 is the same as the notation in the second and third rows of Table 2—they refer to the same objects that can be defined using both Equations (27) and (34).

Part 1: Decomposing $\Omega_{\ell+1}$ into small subdomains

The purpose of this section is to define a set of subdomains that will act as the primary building block used throughout the remainder of the proof, and to clarify some of the characteristics of these subdomains. The results presented in this part are mostly technical and intermediate results, but are necessary to rigorously characterize these domains. To understand the remainder of the document, the following key takeaway should be understood.

Table 3 General and shorthand notation corresponding to Eq. (34) that will be used extensively in the following sections for different choices of $Y \subset \Omega$ and $s \in \{0, 1\}$

Sub-domain and levels	Notation for (34)		
$Y \subset \Omega, s \in \{0, 1\}$	$\mathcal{B}_{\ell+s, \ell+1}^{\mathbf{j}}$	$\mathcal{X}_{\ell+s, \ell+1}^{\mathbf{j}}$	$\mathcal{G}_{\ell+s, \ell+1}(Y)$
$Y = \Omega_{\ell+1}, s = 0$	$\mathcal{B}_{\ell, \ell+1}^{\mathbf{j}}$	$\mathcal{X}_{\ell, \ell+1}^{\mathbf{j}}$	$\mathcal{G}_{\ell, \ell+1}$
$Y = \Omega_{\ell+1}, s = 1$	$\mathcal{B}_{\ell+1, \ell+1}^{\mathbf{j}}$	$\mathcal{X}_{\ell+1, \ell+1}^{\mathbf{j}}$	$\mathcal{G}_{\ell+1, \ell+1}$

Observe that the shorthand notation in the second and third rows above is the same as the notation in the second row of Table 2

Key takeaway from Part 1:

The domain $\Omega_{\ell+1}$ can be decomposed into smaller subdomains, denoted $\Omega_{\ell+1}^{\mathbf{j}}(\mathbf{i})$ (Lemma 4.9), which are all topological balls (Proposition 4.10).

The smaller subdomains $\Omega_{\ell+1}^{\mathbf{j}}(\mathbf{i})$ referenced above will be defined via unions of supports of certain 0-form B-splines. To proceed in a rigorous manner, we need to introduce some new notation. However, we would like to emphasize that this notation—specifically, the notation in (35)–(39)—is only useful for the intermediate results that appear in *Part 1*; it is never explicitly needed in *Part 2* and *Part 3*. Therefore, the reader need only understand this new notation insofar as it is necessary to understand the above key takeaway. To aid in comprehension, representative concepts from this part are illustrated in Fig. 2. The reader may find it useful to refer to this figure as new ideas and notation are introduced.

We start by defining extended knot domains for each parametric direction as

$$\lambda_{\mathbf{i}}^{\mathbf{j}} := \prod_{k=1}^n \widehat{\Xi}[i_k]_{\ell, k}^{j_k}, \tag{35}$$

where the extended univariate knot domains $\widehat{\Xi}[i_k]_{\ell, k}^{j_k}$ are defined as

$$\widehat{\Xi}[i_k]_{\ell, k}^{j_k} := (\xi_{i_k, \ell, k}, \xi_{i_k + p(\ell, k) - j_k + 2, \ell, k}) \subset \mathbb{R}. \tag{36}$$

It should be noted that when $\mathbf{j} = \mathbf{1}$, then the extended knot domain $\lambda_{\mathbf{i}}^{\mathbf{j}}$ is equal to support of a 0-form B-spline with the same index, i.e.,

$$\lambda_{\mathbf{i}}^{\mathbf{1}} = \text{supp}(\alpha_{\mathbf{i}}).$$

With $\mathbf{j} = (j_1, j_2, \dots, j_n)$, we will denote the set of all potential extended local knot domains as

$$\mathbb{X}_{\ell}^{\mathbf{j}} = \left\{ \lambda_{\mathbf{i}}^{\mathbf{j}} : 1 \leq i_k \leq m(\ell, k) + j_k - 1, k = 1, 2, \dots, n \right\}, \tag{37}$$

Remark 4.3 For any practical numerical analysis problem, one would pick spline spaces such that $m_{(\ell,k)} \geq 2$ for all k and ℓ , thus making the set $\mathbb{X}_\ell^{\mathbf{j}}$ non-empty. We therefore assume that $m_{(\ell,k)} \geq 2$ for the rest of the document. However, for completeness we comment here on the special case when $m_{(\ell,k)} = 1$ for at least one k —this will mean $\mathbb{X}_\ell^{\mathbf{j}}$ is an empty set when $j_k = 0$. In such cases, the results of this work still hold but the proofs (which use finite induction on the number of parametric dimensions) would need to be modified to omit the directions where $m_{(\ell,k)} = 1$ since the inductive argument holds automatically in such directions. To keep notation clean from this special case, we thus assume that $m_{(\ell,k)} \geq 2$ henceforth.

Next, we define certain index sets associated to those extended knot domains. For any $\alpha_{\bar{\mathbf{i}}} \in \mathcal{B}_\ell^0$, define $\mathbb{I}_\ell^{\mathbf{j}}(\bar{\mathbf{i}})$ as the set of indices of \mathbf{j} -extended knot domains that are index-space neighbours of $\alpha_{\bar{\mathbf{i}}}$,

$$\mathbb{I}_\ell^{\mathbf{j}}(\bar{\mathbf{i}}) := \{ \mathbf{i} : j_k - 1 \leq i_k - \bar{i}_k \leq 0, k = 1, \dots, n \}. \tag{38}$$

We use the convention that, if $\mathbf{i} \in \mathbb{I}_\ell^{\mathbf{j}}(\bar{\mathbf{i}})$ is such that any $i_k \leq 0$ or $i_k \geq m_{(\ell,k)} + j_k$, then $\lambda_{\mathbf{i}}^{\mathbf{j}} := \emptyset$. Then, if $\mathbf{i} \in \mathbb{I}_\ell^{\mathbf{j}}(\bar{\mathbf{i}})$ then for $\lambda_{\mathbf{i}}^{\mathbf{j}} \neq \emptyset$, $\lambda_{\mathbf{i}}^{\mathbf{j}} \supseteq \text{supp}(\alpha_{\bar{\mathbf{i}}})$ for any \mathbf{j} ; the converse is not true in general. Moreover, $\mathbb{I}_\ell^0(\bar{\mathbf{i}})$ has cardinality $\leq 2^n$ (the inequality holding only when $\bar{\mathbf{i}}$ corresponds to a boundary-adjacent zero form B-spline) while $\mathbb{I}_\ell^1(\bar{\mathbf{i}})$ has cardinality 1.

Denote with $\mathbb{I}_{\ell,\ell+1}^{\mathbf{j}}$ the union of such index-space neighbours for all $\alpha_{\bar{\mathbf{i}}} \in \mathcal{B}_{\ell,\ell+1}^0$, i.e.,

$$\mathbb{I}_{\ell,\ell+1}^{\mathbf{j}} := \bigcup_{\alpha_{\bar{\mathbf{i}}} \in \mathcal{B}_{\ell,\ell+1}^0} \mathbb{I}_\ell^{\mathbf{j}}(\bar{\mathbf{i}}). \tag{39}$$

Next, if \mathbf{i} is the index of an index-space neighbour, define $D_{\ell,\ell+1}^{\mathbf{j}}(\mathbf{i})$ as the set containing supports of 0-form B-splines that are supported on $\Omega_{\ell+1}$ as well as the given index-space neighbour,

$$D_{\ell,\ell+1}^{\mathbf{j}}(\mathbf{i}) := \{ \bar{\mathbf{i}} : \text{supp}(\alpha_{\bar{\mathbf{i}}}) \subset \Omega_{\ell+1} \text{ and } j_k - 1 \leq i_k - \bar{i}_k \leq 0, k = 1, \dots, n \}. \tag{40}$$

Observe that $D_{\ell,\ell+1}^1(\mathbf{i})$ has cardinality ≤ 1 while $D_{\ell,\ell+1}^0(\mathbf{i})$ has cardinality $\leq 2^n$.

Remark 4.4 Since each 1-extended knot domain can be interpreted as the support of a zero form B-spline, notice that $\mathbb{I}_{\ell,\ell+1}^{\mathbf{j}}$ and $D_{\ell,\ell+1}^{\mathbf{j}}(\mathbf{i})$ are sort of “inverses” of each other—the former contains the indices of all \mathbf{j} -extended knot domains that are index-space neighbours of zero form B-splines supported on $\Omega_{\ell+1}$, while the latter contains the indices of all zero form B-splines supported on $\Omega_{\ell+1}$ for which a given \mathbf{j} -extended knot domain is an index-space neighbour. This observation is encapsulated in Lemma 4.7 below.

Lemma 4.7 *Let \mathbf{i} and $\bar{\mathbf{i}}$ be such that, for all k ,*

$$j_k - 1 \leq i_k - \bar{i}_k \leq 0.$$

If $\alpha_{\bar{\mathbf{i}}} \in \mathcal{B}_{\ell, \ell+1}^0$, then $\mathbf{i} \in \mathbb{I}_{\ell, \ell+1}^{\mathbf{j}}$ and $\bar{\mathbf{i}} \in D_{\ell, \ell+1}^{\mathbf{j}}(\mathbf{i})$.

Proof By definition, $\lambda_{\bar{\mathbf{i}}}^{\mathbf{j}}$ is an index space neighbour of $\alpha_{\bar{\mathbf{i}}}$ and the latter is supported on $\Omega_{\ell+1}$, thus implying $\mathbf{i} \in \mathbb{I}_{\ell, \ell+1}^{\mathbf{j}}$. Clearly, $\lambda_{\bar{\mathbf{i}}}^{\mathbf{j}} = \text{supp}(\alpha_{\bar{\mathbf{i}}}) \subset \Omega_{\ell+1}$, and thus $\bar{\mathbf{i}} \in D_{\ell, \ell+1}^{\mathbf{j}}(\mathbf{i})$. □

The union of all $\mathbf{1}$ -extended knot domains with indices in $D_{\ell, \ell+1}^{\mathbf{j}}(\mathbf{i})$ forms a subset of $\Omega_{\ell+1}$, we denote this subset with $\Omega_{\ell+1}^{\mathbf{j}}(\mathbf{i})$,

$$\Omega_{\ell+1} \supset \Omega_{\ell+1}^{\mathbf{j}}(\mathbf{i}) := \bigcup_{\bar{\mathbf{i}} \in D_{\ell, \ell+1}^{\mathbf{j}}(\mathbf{i})} \text{supp}(\alpha_{\bar{\mathbf{i}}}) \tag{41}$$

Here, if $D_{\ell, \ell+1}^{\mathbf{j}}(\mathbf{i}) = \emptyset$, it implies that $\Omega_{\ell+1}^{\mathbf{j}}(\mathbf{i}) = \emptyset$.

Figure 2 depicts a potential refinement scenario on a spline space of two levels and highlights interpretations of the aforementioned notation. Particularly of consequence are the domains, $\Omega_{\ell+1}^{\mathbf{j}}(\mathbf{i})$, which in the following results are shown to be topological balls when non-empty, the unions of which can reconstruct $\Omega_{\ell+1}$.

Corollary 4.8 *$\Omega_{\ell+1}^{\mathbf{j}}(\mathbf{i})$ is non-empty if and only if $\mathbf{i} \in \mathbb{I}_{\ell, \ell+1}^{\mathbf{j}}$.*

Proof If $\mathbf{i} \in \mathbb{I}_{\ell, \ell+1}^{\mathbf{j}}$, there is a 0-form B-spline $\alpha_{\bar{\mathbf{i}}}$ supported on $\lambda_{\bar{\mathbf{i}}}^{\mathbf{j}} \cap \Omega_{\ell+1}$ such that, for all k ,

$$j_k - 1 \leq i_k - \bar{i}_k \leq 0.$$

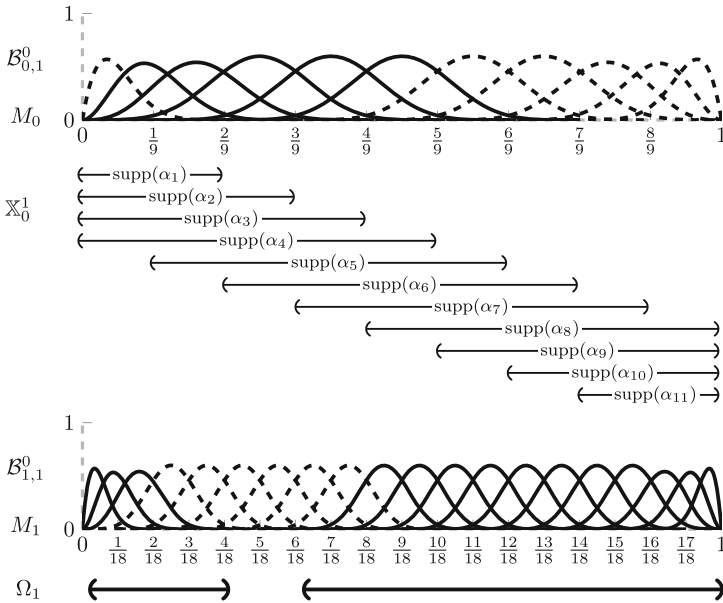
Then, from Lemma 4.7, $\Omega_{\ell+1}^{\mathbf{j}}(\mathbf{i}) \supset \text{supp}(\alpha_{\bar{\mathbf{i}}})$.

Conversely, if $\Omega_{\ell+1}^{\mathbf{j}}(\mathbf{i})$ is non-empty, there exists some $\alpha_{\bar{\mathbf{i}}} \in \mathcal{B}_{\ell, \ell+1}^0$ with $\bar{\mathbf{i}} \in D_{\ell, \ell+1}^{\mathbf{j}}(\mathbf{i})$. Then by definition of $\bar{\mathbf{i}} \in D_{\ell, \ell+1}^{\mathbf{j}}(\mathbf{i})$, the inequality of Lemma 4.7 is satisfied, meaning that $\mathbf{i} \in \mathbb{I}_{\ell, \ell+1}^{\mathbf{j}}$. □

Lemma 4.9 *The domain $\Omega_{\ell+1}$ can be constructed by taking the union of $\Omega_{\ell+1}^{\mathbf{j}}(\mathbf{i})$ over all $\mathbf{i} \in \mathbb{I}_{\ell, \ell+1}^{\mathbf{j}}$ for any \mathbf{j} , i.e.,*

$$\Omega_{\ell+1} = \bigcup_{\mathbf{i} \in \mathbb{I}_{\ell, \ell+1}^{\mathbf{j}}} \Omega_{\ell+1}^{\mathbf{j}}(\mathbf{i}). \tag{42}$$

Proof The claim follows from Lemma 4.7 and Corollary 4.8. □



\bar{i}	$\mathbb{I}_0^0(\bar{i})$	$\mathbb{I}_1^1(\bar{i})$	i	$D_{0,1}^0(i)$	$\Omega_1^0(i)$	$D_{0,1}^1(i)$	$\Omega_1^1(i)$
1	{0,1}	{1}	1	{1}	supp(α_1)	{1}	supp(α_1)
2	{1,2}	{2}	2	\emptyset	\emptyset	\emptyset	\emptyset
3	{2,3}	{3}	3	\emptyset	\emptyset	\emptyset	\emptyset
4	{3,4}	{4}	4	\emptyset	\emptyset	\emptyset	\emptyset
5	{4,5}	{5}	5	\emptyset	\emptyset	\emptyset	\emptyset
6	{5,6}	{6}	6	{7}	supp(α_7)	\emptyset	\emptyset
7	{6,7}	{7}	7	{7,8}	supp(α_7) \cup supp(α_8)	{7}	supp(α_7)
8	{7,8}	{8}	8	{8,9}	supp(α_8) \cup supp(α_9)	{8}	supp(α_8)
9	{8,9}	{9}	9	{9,10}	supp(α_9) \cup supp(α_{10})	{9}	supp(α_9)
10	{9,10}	{10}	10	{10,11}	supp(α_{10}) \cup supp(α_{11})	{10}	supp(α_{10})
11	{10,11}	{11}	11	{11}	supp(α_{11})	{11}	supp(α_{11})

$\mathbb{I}_{0,1}^0$	{0, 1} \cup {6, 7} \cup {7, 8} \cup {8, 9} \cup {9, 10} \cup {10, 11}
$\mathbb{I}_{0,1}^1$	{1} \cup {7} \cup {8} \cup {9} \cup {10} \cup {11}

Fig. 2 This figure shows the quantities defined throughout *Part I* of Sect. 4.2 by taking a 2-level spline space as an example. We consider the level-0 knot vector as $\Xi_{0,1} = \{0, 0, 0, 0, \frac{1}{9}, \frac{2}{9}, \frac{3}{9}, \frac{4}{9}, \frac{5}{9}, \frac{6}{9}, \frac{7}{9}, \frac{8}{9}, 1, 1, 1, 1\}$, and the level-1 knot vector $\Xi_{1,1}$ is defined through dyadic refinement. The associated 0-form B-splines, $B_{0,1}^0$ and $B_{1,1}^0$, are shown above. In particular, with the refinement domain chosen as $\Omega_1 = (0, \frac{2}{9}) \cup (\frac{1}{3}, 1)$, inactive and active splines on both levels are displayed in dashed and solid lines, respectively. Tabulated below these figures are sets $\mathbb{I}_0^0(\bar{i})$ and $\mathbb{I}_1^1(\bar{i})$ that define the index-space neighbors of splines on level 0; index sets $D_{0,1}^0(i)$ and $D_{0,1}^1(i)$ for 1-extended knot domains supported on Ω_1 ; respectively, their associated subsets $\Omega_1^0(i)$ and $\Omega_1^1(i)$; and the unions of index-space neighbors in $\mathbb{I}_{0,1}^0$ and $\mathbb{I}_{0,1}^1$. This example also shows how $\Omega_1^0(i)$ can be larger than the support of a single 0-form, as is the case for $\Omega_1^0(7)$

Proposition 4.10 *If $\mathbf{i} \in \mathbb{I}_{\ell, \ell+1}^j$ then $\Omega_{\ell+1}^j(\mathbf{i})$ is a ball.*

Proof As $\mathbf{i} \in \mathbb{I}_{\ell, \ell+1}^j$, $\Omega_{\ell+1}^j(\mathbf{i})$ is not empty. In fact, by definition, $\Omega_{\ell+1}^j(\mathbf{i})$ is equal to the union of the supports of at most 2^n 0-form B-splines. Specifically, $\Omega_{\ell+1}^j(\mathbf{i})$ is the union of one or more members of the set

$$\left\{ \prod_{k=1}^n \widehat{\Xi}[i_k]_{\ell, k}^1 : \forall k, 0 \leq \bar{i}_k - i_k \leq 1 \right\}.$$

Observe that all members of the above set are n -dimensional hypercubes (and thus are all convex) and contain $\text{supp}(\zeta)$, where ζ is an n -form B-spline defined as

$$\zeta := \prod_{k=1}^n \Xi[i_k + 1]_{\ell, k}^1.$$

Therefore, $\Omega_{\ell+1}^j(\mathbf{i})$ is open and star-shaped with respect to any point in $\text{supp}(\zeta)$. As a result [14], $\Omega_{\ell+1}^j(\mathbf{i})$ is an open ball. □

Part 2: Cohomologically equivalent spline complexes on the subdomains

Similarly to **Part 1**, the results here are mostly technical intermediate results. We therefore start by summarizing the key takeaway that will be useful for **Part 3**. Given this result, the reader can skip ahead if desired.

Key takeaway from Part 2:

Not only are $\Omega_{\ell+1}^j(\mathbf{i})$ topologically trivial domains, but the level ℓ and $\ell + 1$ splines supported on them also form cohomologically equivalent subcomplexes (Corollary 4.15).

Thus, the results of **Part 1** and **Part 2** can together be summarized as follows: the domain $\Omega_{\ell+1}$ can be decomposed into topologically trivial subdomains and, on each such subdomain, the level ℓ and $\ell + 1$ spline subcomplexes are cohomologically equivalent.

Lemma 4.11 *If $B \subset A$, then*

$$\begin{aligned} \mathcal{B}_{\ell+s, \ell+1}^j(B) &\subset \mathcal{B}_{\ell+s, \ell+1}^j(A), \\ \mathcal{X}_{\ell+s, \ell+1}^j(B) &\subset \mathcal{X}_{\ell+s, \ell+1}^j(A), \\ \mathcal{G}_{\ell+s, \ell+1}(B) &\subset \mathcal{G}_{\ell+s, \ell+1}(A). \end{aligned}$$

Proof The claim follows from the definitions of the three objects. □

Proposition 4.12 *Let $A = \Omega_{\ell+1}^j(\mathbf{i})$ and $s = 0$ or 1 . A is empty if and only if $\mathcal{G}_{\ell+s, \ell+1}(A)$ is empty. Moreover, if A is a topological ball then so is $\mathcal{G}_{\ell+s, \ell+1}(A)$.*

Proof By definition of $A = \Omega_{\ell+1}^{\mathbf{j}}$ and $\mathcal{G}_{\ell+s,\ell+1}(A)$, one being empty implies the other must be empty.

Then assume that A is non-empty and thus is a ball, as shown in Corollary 4.8 and Proposition 4.10. We proceed as in Proposition 4.10. Recall from that proof that A is the union of the supports of at most 2^n 0-form B-splines. Then, for each such zero form α , and with ζ defined to be the n -form B-spline used in the proof of Proposition 4.10, $\text{supp}(\zeta) \subset \text{supp}(\alpha) \subset A$. Observe that each $\mathcal{G}_{\ell+s,\ell+1}(\text{supp}(\alpha))$ is an n -dimensional hypercube (and thus convex) and, from Lemma 4.11, contains $\mathcal{G}_{\ell+s,\ell+1}(\text{supp}(\zeta))$. Therefore, as before, $\mathcal{G}_{\ell+s,\ell+1}(A)$ is open and star-shaped with respect to any point in $\mathcal{G}_{\ell+s,\ell+1}(\text{supp}(\zeta))$, and is thus an open ball. \square

Using the above and given a domain A , we now define spline complex $\mathcal{X}_{\ell+s,\ell+1}(A)$, $s = 0, 1$, as

$$\mathcal{X}_{\ell+s,\ell+1}(A) : \mathcal{X}_{\ell+s,\ell+1}^0(A) \xrightarrow{d} \mathcal{X}_{\ell+s,\ell+1}^1(A) \xrightarrow{d} \dots \xrightarrow{d} \mathcal{X}_{\ell+s,\ell+1}^n(A). \quad (43)$$

Lemma 4.13 shows that, for certain domains A , the complex $\mathcal{X}_{\ell+s,\ell+1}(A)$ is the same as $\mathcal{X}_{\ell+s}(A)$. Moreover, Corollary 4.14 shows that these complexes are exact.

Lemma 4.13 *Let $A \subset \Omega_{\ell+1}$ is a union of supports of a subset of $\mathcal{B}_{\ell,\ell+1}^0$ such that for any $\phi \in \mathcal{B}_{\ell+s}^{\mathbf{j}}(A)$, $s = 0, 1$, there exists $\alpha \in \mathcal{B}_{\ell,\ell+1}^0(A)$ such that $\text{supp}(\phi) \subset \text{supp}(\alpha)$. Then, for all j ,*

$$\mathcal{X}_{\ell+s}^j(A) = \mathcal{X}_{\ell+s,\ell+1}^j(A). \quad (44)$$

Proof It is clear that $\mathcal{X}_{\ell+s,\ell+1}^j(A) \subset \mathcal{X}_{\ell+s}^j(A)$ from the definitions. For the inclusion in the other direction, notice that if there is a B-spline $\phi \in \mathcal{X}_{\ell+s}^j(A)$, then there exists a \mathbf{j} , $|\mathbf{j}| = j$, such that $\phi \in \mathcal{B}_{\ell+s}^{\mathbf{j}}(A)$. However, by the assumption on A , there exists an $\alpha \in \mathcal{B}_{\ell,\ell+1}^0(A)$ such that $\text{supp}(\phi) \subset \text{supp}(\alpha)$. Then, by definition, $\phi \in \mathcal{X}_{\ell+s,\ell+1}^j(A)$. \square

When $\mathcal{X}_{\ell+s,\ell+1}(A) = \mathcal{X}_{\ell+s}(A)$ for some choice of A , then we will denote the j -cohomology of both $\mathcal{X}_{\ell+s,\ell+1}(A)$ and $\mathcal{X}_{\ell+s}(A)$ with $H_{\ell+s}^{(j)}(A)$. One such choice is when A is a union of supports of splines in $\mathcal{B}_{\ell,\ell+1}^0$, as in Lemma 4.13.

Corollary 4.14 *For $A = \Omega_{\ell+1}^{\mathbf{j}} \neq \emptyset$, $\mathcal{X}_{\ell+s,\ell+1}(A)$ is exact, $s = 0, 1$, i.e.,*

$$H_{\ell}^{(j)}(A) = H_{\ell+1}^{(j)}(A) = \begin{cases} 0, & j = 0, 1, \dots, n - 1, \\ \mathbb{R}, & j = n. \end{cases} \quad (45)$$

Proof The proof follows the same argument as in [12, Corollary 5.12] and uses standard results from homology and cohomology. From Propositions 4.10 and 4.12 and direct

computation [15, Chapter 2],

$$H_{(n-j)}(A) \approx H_{(n-j)}(\mathcal{G}_{\ell,\ell+1}(A)) \approx H_{(n-j)}(\mathcal{G}_{\ell+1,\ell+1}(A)) \approx \begin{cases} \mathbb{R}, & j = n, \\ 0, & \text{otherwise.} \end{cases}$$

By the correspondence between the tensor-product splines and their Greville grids [12], we also have for $s = 0, 1$,

$$H_{\ell+s}^{(j)}(A) \approx H^{(j)}(\mathcal{G}_{\ell+s,\ell+1}(A), \partial\mathcal{G}_{\ell+s,\ell+1}(A)), \quad s = 0, 1.$$

Then, the claim follows from the Lefschetz duality theorem [15, Theorem 3.43] which states that

$$H^{(j)}(\mathcal{G}_{\ell+s,\ell+1}(A), \partial\mathcal{G}_{\ell+s,\ell+1}(A)) \approx H_{(n-j)}(\mathcal{G}_{\ell,\ell+1}(A)), \quad s = 0, 1.$$

□

Corollary 4.15 *Let $A = \Omega_{\ell+1}^{\mathbf{j}}$ for any multi-index \mathbf{i} . Then, the inclusion operator $\iota_{\ell,\ell+1} : \mathcal{X}_{\ell,\ell+1}(A) \rightarrow \mathcal{X}_{\ell+1,\ell+1}(A)$ induces an isomorphism on cohomology.*

Proof If $A \neq \emptyset$, this follows directly from Corollary 4.14. Otherwise, $A = \emptyset$ and the result holds trivially. □

Remark 4.5 As was done in [12], it is also possible to show Corollary 4.15 by defining projection operators $\widehat{\Pi}^j : \mathcal{X}_{\ell+1,\ell+1}^j(A) \rightarrow \mathcal{X}_{\ell,\ell+1}^j(A)$ via the following problem,

$$(\widehat{\Pi}^j f, d^{j-1} g) = (f, d^{j-1} g), \quad \forall g \in \mathcal{X}_{\ell,\ell+1}^{j-1}(A), \tag{46a}$$

$$(d^j \widehat{\Pi}^j f, d^j g) = (d^j f, d^j g), \quad \forall g \in \mathcal{X}_{\ell,\ell+1}^j(A), \quad j = 0, \dots, n-1, \tag{46b}$$

$$\int_A \widehat{\Pi}^n f = \int_A f. \tag{46c}$$

In the above system, the first sub-equation helps determine the part of $\widehat{\Pi}^j f$ that is exact. Then, from Propositions 4.10 and 4.12, the remaining part of $\widehat{\Pi}^j f$ that needs to be determined is co-exact for $j = 0, \dots, n-1$, and harmonic for $j = n$; these are respectively determined by the second (recall that we are working with homogeneous boundary conditions here) and third sub-equations.

Part 3: Piecing together the subdomain complexes

We now piece-together the subdomain complexes to show that the hierarchical spline complex is exact, given that an additional assumption (Assumption 3) is satisfied. We get to this final result (Theorem 4.23) by building upon the key takeaways from **Part 1** and **Part 2** that were highlighted earlier, and we again summarize key results from this section in the following.

Key takeaway from Part 3:

Theorem 4.23 is the main result here. The hierarchical complex $\mathcal{W}_{\ell+1}$, which is obtained from \mathcal{W}_ℓ by refining $\Omega_{\ell+1}$, can be equivalently constructed via an inductive process whereby certain groups of $\Omega_{\ell+1}^{\mathbf{j}}(\mathbf{i})$ are successively refined. Theorem 4.23 states that, given Assumption 3, the cohomological structure of the complex stays the same at each step of this latter inductive process.

Main steps in the inductive proof:

Lemma 4.17 helps understand the relationship between unions and intersections of the level- $(\ell + 1)$ refinement domain at consecutive steps in the inductive process. Lemmas 4.18 and 4.20 show that the level ℓ and $\ell + 1$ spline complexes supported on such unions and intersections are well-behaved. Finally, Propositions 4.21 and 4.22 establish the claimed cohomology-invariance during the inductive process.

Definition 4.1 (*An $(n - 1, \ell + 1)$ -intersection*) Let $\alpha_{\bar{\mathbf{i}}}, \alpha_{\bar{\mathbf{i}}+\Delta\bar{\mathbf{i}}} \in \mathcal{B}_\ell^0(\Omega_{\ell+1})$ and, without loss of generality, assume that $\Delta\bar{\mathbf{i}}$ is component-wise non-negative. We say that $\alpha_{\bar{\mathbf{i}}}$ and $\alpha_{\bar{\mathbf{i}}+\Delta\bar{\mathbf{i}}}$ share an $(n - 1, \ell + 1)$ -intersection if there exists $\bar{\mathbf{i}}', k_0$ such that

$$\overline{\text{supp}}(\alpha_{\bar{\mathbf{i}}}) \cap \overline{\text{supp}}(\alpha_{\bar{\mathbf{i}}+\Delta\bar{\mathbf{i}}}) \supseteq \bigtimes_{k=1}^n I_k, \tag{47a}$$

$$I_k := \begin{cases} \left(\xi_{\bar{\mathbf{i}}', \ell+1, k}, \xi_{\bar{\mathbf{i}}'+p(\ell+1, k), \ell+1, k} \right), & k \neq k_0, \\ \{ \xi_{\bar{\mathbf{i}}', \ell+1, k} \}, & k = k_0. \end{cases} \tag{47b}$$

If needed, we will say that $\alpha_{\bar{\mathbf{i}}}$ and $\alpha_{\bar{\mathbf{i}}+\Delta\bar{\mathbf{i}}}$ share an $(n - 1, \ell + 1)$ -intersection w.r.t. the direction k_0 .

Definition 4.2 (*A chain*) Let $\alpha_{\bar{\mathbf{i}}}, \alpha_{\bar{\mathbf{i}}+\Delta\bar{\mathbf{i}}} \in \mathcal{B}_{\ell, \ell+1}^0$. There is said to be a chain between $\alpha_{\bar{\mathbf{i}}}$ and $\alpha_{\bar{\mathbf{i}}+\Delta\bar{\mathbf{i}}}$ if there is some positive integer r and a set of B-splines $\alpha_{\bar{\mathbf{i}}+\Delta\bar{\mathbf{i}}^l} \in \mathcal{B}_{\ell, \ell+1}^0, l = 0, \dots, r$ such that

- $\Delta\bar{\mathbf{i}}_0 = \mathbf{0}, \Delta\bar{\mathbf{i}}_r = \Delta\bar{\mathbf{i}}$;
- $\Delta\bar{\mathbf{i}}_l - \Delta\bar{\mathbf{i}}_{l-1}$ is zero in all components but one, and the sum of all components is equal to ± 1 for all $l = 1, \dots, r$.

Definition 4.3 (*A shortest chain*) Let $\alpha_{\bar{\mathbf{i}}}, \alpha_{\bar{\mathbf{i}}+\Delta\bar{\mathbf{i}}} \in \mathcal{B}_{\ell, \ell+1}^0$ and, without loss of generality, assume that $\Delta\bar{\mathbf{i}}$ is component-wise non-negative. A chain between $\alpha_{\bar{\mathbf{i}}}$ and $\alpha_{\bar{\mathbf{i}}+\Delta\bar{\mathbf{i}}}$ is a shortest chain if

- $r := \sum_k \Delta\bar{\mathbf{i}}_k$;
- $\Delta\bar{\mathbf{i}}_l - \Delta\bar{\mathbf{i}}_{l-1}$ is component-wise non-negative, with the sum of all components being equal to 1 for all $l = 1, \dots, r$.

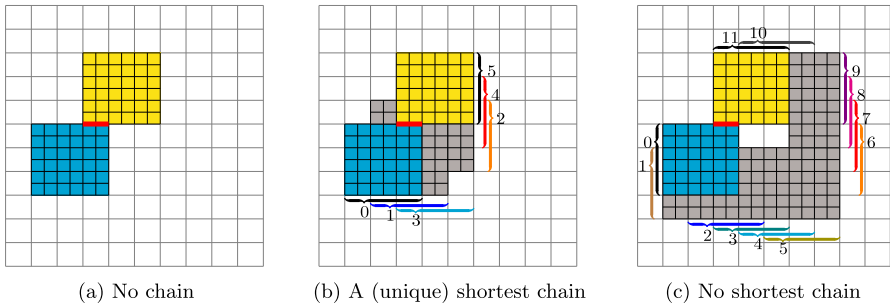


Fig. 3 In the above figures, we consider two levels of a maximally regular hierarchical spline space defined using $p_{(\ell,k)} = 2$ for all ℓ and k . The shaded cells (of any colour) constitute $\Omega_{\ell+1}$. In particular, the two biquadratic 0-form B-splines $\alpha_{\bar{i}}, \alpha_{\bar{i}+(2,3)} \in \mathcal{B}_{\ell,\ell+1}^0$ share an $(n - 1, \ell + 1)$ intersection, depicted in red. Here, $\alpha_{\bar{i}}$ is on the lower-left and its support is shaded blue, while $\alpha_{\bar{i}+(2,3)} \in \mathcal{B}_{\ell,\ell+1}^0$ is on the upper-right and its support is shaded yellow; the rest of $\Omega_{\ell+1}$ is shown in grey. In figure (a), there are no other B-splines in $\mathcal{B}_{\ell,\ell+1}^0$, and thus no chain of indices traversing from one to the other. In figure (b), the refinement pattern supports a shortest chain between the 0-form B-splines, with numbers indicating the magnitude of $\Delta \bar{i}_l$, as in Definition 4.3. On the right, the refinement supports a chain, with numbers also indicating the number l in $\Delta \bar{i}_l$, but the chain is not a shortest chain

Remark 4.6 We would like to highlight a notational subtlety here that the reader should keep in mind: bold fonts (with or without subscripts) are used to denote multi-indices, while normal font (with subscripts) is used to denote components of the multi-indices. For instance, see Definition 4.3 where $\Delta \bar{i}, \Delta \bar{i}_{l-1}$ and $\Delta \bar{i}_l$ are all multi-indices, while $\Delta \bar{i}_k$ are the components of the multi-index $\Delta \bar{i}$.

Lemma 4.16 *Let there be a shortest chain between $\alpha_{\bar{i}}, \alpha_{\bar{i}+\Delta \bar{i}} \in \mathcal{B}_{\ell}^0(\Omega_{\ell+1})$. Then the closure of the support of any B-spline in the shortest chain contains $\overline{\text{supp}}(\alpha_{\bar{i}}) \cap \overline{\text{supp}}(\alpha_{\bar{i}+\Delta \bar{i}})$.*

Assumption 3 The following hold.

(a) Let $\alpha_{\bar{i}}, \alpha_{\bar{i}+\Delta \bar{i}} \in \mathcal{B}_{\ell}^0(\Omega_{\ell+1})$. If $\alpha_{\bar{i}}$ and $\alpha_{\bar{i}+\Delta \bar{i}}$ share an $(n - 1, \ell + 1)$ -intersection, then there exists a shortest chain between them.

(b) Let $\mathcal{A} \subset \mathcal{B}_{\ell}^0(\Omega_{\ell+1})$ and let $\phi \in \mathcal{B}_{\ell+s}^j(\Omega_{\ell+1})$, $s = 0, 1$, be such that $\text{supp}(\phi) \subset \bigcup_{\alpha \in \mathcal{A}} \overline{\text{supp}}(\alpha)$. Then there exists $\alpha_0 \in \mathcal{B}_{\ell}^0(\Omega_{\ell+1})$ such that $\text{supp}(\phi) \subset \text{supp}(\alpha_0)$ and $\text{supp}(\alpha_0)$ is contained in the smallest axis-aligned bounding box that contains $\bigcup_{\alpha \in \mathcal{A}} \text{supp}(\alpha)$.

Figure 3 illustrates the concept of $(n - 1, \ell + 1)$ intersections, chains, and shortest chains between two 0-forms under different refinement scenarios. Of these configurations, only that of subfigure 3(b) satisfies the conditions of Assumption 3. Assumption 3 also guarantees that Lemma 4.13 holds for the refined domains employed in this work.

For this final part of the proof and for given $0 \leq \ell \leq L - 1$, define the following “slices” of $\Omega_{\ell+1}$, where $\mathbf{i}, \mathbf{j}, \mathbf{r}$ and \mathbf{m} are n -tuples,

$$S_i^j[\mathbf{m}] := \bigcup_{r_1=0}^{m_1} \cdots \bigcup_{r_n=0}^{m_n} \Omega_{\ell+1}^j(\mathbf{i} + \mathbf{r}), \tag{48}$$

and recall that each $\Omega_{\ell+1}^j(\mathbf{i} + \mathbf{r}) = \emptyset$ or is a ball by Corollary 4.8 and Proposition 4.10. Note that, from Lemma 4.9, if $m_i = m_{(\ell,i)}$ for all i then

$$S_1^j[\mathbf{m}] = \bigcup_{r_1=0}^{m_{(\ell,1)}} \cdots \bigcup_{r_n=0}^{m_{(\ell,n)}} \Omega_{\ell+1}^j(\mathbf{1} + \mathbf{r}) = \Omega_{\ell+1}. \tag{49}$$

Lemma 4.17 *Let Assumption 3 hold. For a fixed $1 \leq k \leq n$, let δ_k be an n -tuple with the value 1 in index k and 0 elsewhere, and let \mathbf{i}, \mathbf{j} and \mathbf{m} be given. Then, with $\bar{\mathbf{r}} := (r_1, \dots, r_{k-1}, 0, r_{k+1}, \dots, r_n)$ and with*

$$\begin{aligned} A_i^j &:= S_i^j[\mathbf{m}], \\ B_i^j &:= \bigcup_{r_1=0}^{m_1} \cdots \bigcup_{r_{k-1}=0}^{m_{k-1}} \bigcup_{r_{k+1}=0}^{m_{k+1}} \cdots \bigcup_{r_n=0}^{m_n} \Omega_{\ell+1}^j(\mathbf{i} + \bar{\mathbf{r}} + (m_k + 1)\delta_k), \\ C_i^j &:= S_i^j[\mathbf{m} + \delta_k], \end{aligned}$$

the following hold,

$$A_i^j \cap B_i^j \supset B_i^{j+\delta_k} \quad \text{for } j_k = 0, \tag{50}$$

$$A_i^j \cup B_i^j = C_i^j \quad \text{for } j_k = 0, 1. \tag{51}$$

Proof Given r_k , let $\mathbf{r} := \bar{\mathbf{r}} + r_k \delta_k$. Then, since $\bigcup_{r_k=0}^{m_k+1} = \left(\bigcup_{r_k=0}^{m_k}\right) \cup \left(\bigcup_{r_k=m_k+1}\right)$, the second equality follows from definitions of the domains,

$$\begin{aligned} C_i^j &= \bigcup_{r_1=0}^{m_1} \cdots \bigcup_{r_{k-1}=0}^{m_{k-1}} \bigcup_{r_k=0}^{m_k+1} \bigcup_{r_{k+1}=0}^{m_{k+1}} \cdots \bigcup_{r_n=0}^{m_n} \Omega_{\ell+1}^j(\mathbf{i} + \mathbf{r}) \\ &= \left(\bigcup_{r_1=0}^{m_1} \cdots \bigcup_{r_{k-1}=0}^{m_{k-1}} \bigcup_{r_k=0}^{m_k} \bigcup_{r_{k+1}=0}^{m_{k+1}} \cdots \bigcup_{r_n=0}^{m_n} \Omega_{\ell+1}^j(\mathbf{i} + \mathbf{r}) \right) \\ &\quad \cup \left(\bigcup_{r_1=0}^{m_1} \cdots \bigcup_{r_{k-1}=0}^{m_{k-1}} \bigcup_{r_{k+1}=0}^{m_{k+1}} \cdots \bigcup_{r_n=0}^{m_n} \Omega_{\ell+1}^j(\mathbf{i} + \bar{\mathbf{r}} + (m_k + 1)\delta_k) \right), \\ &= A_i^j \cup B_i^j. \end{aligned}$$

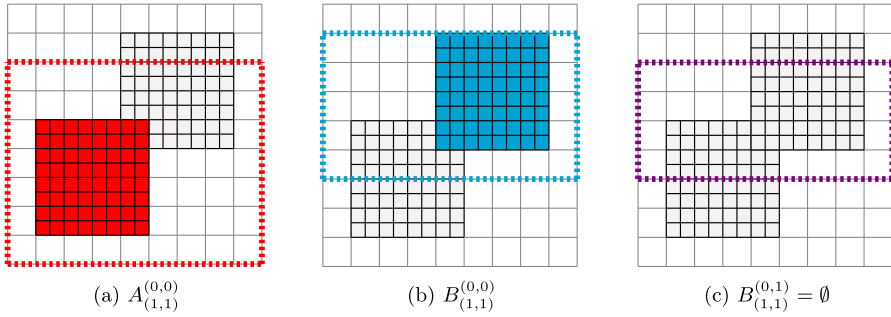


Fig. 4 The above figures correspond to a maximally regular hierarchical spline space defined using $p_{(\ell,k)} = 3$ for all ℓ and k . Here, $m_{(0,k)} = 10$ and $m_{(1,k)} = 19$ for all k . Figures (a), (b) and (c) depict domains A_i^j , B_i^j , and $B_i^{j+\delta_k}$, respectively, as defined in Lemma 4.17 for $k = 2$. Here, dashed lines indicate the extents of 0-form B-splines whose support could potentially contribute to the domain, while the shaded cells of the same color correspond to the actual domain. Greyed-out sections are portions of $\Omega_{\ell+1}$ that are not contained in the referenced domain. This refinement pattern obeys all assumptions of this paper, so the inequality of equation (50) holds and takes the form of $A_i^j \cap B_i^j \neq \emptyset = B_i^{j+\delta_k}$

The inclusion $B_i^{j+\delta_k} \subset A_i^j$ is clear from the definitions so we only need to show the containment $B_i^{j+\delta_k} \subset B_i^j$. Consider a Bézier element contained in $B_i^{j+\delta_k}$. Then, there exists a 0-form B-spline $\alpha_{\bar{i}}$ whose support is contained in $B_i^{j+\delta_k}$ and containing this Bézier element, i.e., $\bar{i} \in D_{\ell,\ell+1}^{j+\delta_k}(\mathbf{i} + \bar{\mathbf{r}} + (m_k + 1)\delta_k)$ for some $\bar{\mathbf{r}}$. Thus, $(\bar{\mathbf{i}} - \mathbf{i} - \bar{\mathbf{r}} - (m_k + 1)\delta_k)$ is a non-negative n -tuple that is component-wise less than or equal to $(\mathbf{1} - \mathbf{j} - \delta_k)$, and thus component-wise less than or equal to $(\mathbf{1} - \mathbf{j})$. Therefore, $\bar{i} \in D_{\ell,\ell+1}^j(\mathbf{i} + \bar{\mathbf{r}} + (m_k + 1)\delta_k)$ and thus $\text{supp}(\alpha_{\bar{i}}) \subset B_i^j$. \square

Remark 4.7 The relationship of equation (50) in Lemma 4.17 may actually be an equality or may be strict, depending on the refinement pattern of $\Omega_{\ell+1}$. Figure 4 depicts one scenario in which the subset relationship is a proper subset relationship because $A_i^j \cap B_i^j$ is not empty but $B_i^{j+\delta_k}$ is. If, however, the two refined 0-form domains of this picture had a shortest chain connecting each other, the subset relationship would actually be an equality.

Lemma 4.18 *Let Assumption 3 hold. For a fixed $1 \leq k \leq n$, let δ_k be an n -tuple with the value 1 in index k and 0 elsewhere, and let \mathbf{i}, \mathbf{j} and \mathbf{m} be given with $j_k = 0$. Then, with $\bar{\mathbf{r}} := (r_1, \dots, r_{k-1}, 0, r_{k+1}, \dots, r_n)$ and with*

$$A_i^j := S_i^j[\mathbf{m}],$$

$$B_i^j := \bigcup_{r_1=0}^{m_1} \dots \bigcup_{r_{k-1}=0}^{m_{k-1}} \bigcup_{r_{k+1}=0}^{m_{k+1}} \dots \bigcup_{r_n=0}^{m_n} \Omega_{\ell+1}^j(\mathbf{i} + \bar{\mathbf{r}} + (m_k + 1)\delta_k),$$

the following holds for $s = 0, 1$,

$$B_{\ell+s,\ell+1}^*(A_i^j) \cap B_{\ell+s,\ell+1}^*(B_i^j) = B_{\ell+s,\ell+1}^*(A_i^j \cap B_i^j) = B_{\ell+s,\ell+1}^*(B_i^{j+\delta_k}). \quad (52)$$

Here, a superscript of $*$ denotes that the statement is true for all sets of B-splines, i.e., for all possible superscripts.

Proof If $\phi \in \mathcal{B}_{\ell+s, \ell+1}^*(A_i^j) \cap \mathcal{B}_{\ell+s, \ell+1}^*(B_i^j)$, then by definition there must exist an n -form $\zeta \in \mathcal{B}_{\ell+1, \ell+1}^1$ and two 0-form B-splines $\alpha_{\bar{i}}, \alpha_{\bar{i}+\Delta\bar{i}} \in \mathcal{B}_{\ell, \ell+1}^0$, such that

$$\begin{aligned} \text{supp}(\zeta) \subset \text{supp}(\phi) \subset \text{supp}(\alpha_{\bar{i}}) \subset A_i^j, \\ \text{supp}(\zeta) \subset \text{supp}(\phi) \subset \text{supp}(\alpha_{\bar{i}+\Delta\bar{i}}) \subset B_i^j. \end{aligned}$$

Without loss of generality, assume that $\Delta\bar{i}$ is component-wise non-negative. The above implies that $\alpha_{\bar{i}}$ and $\alpha_{\bar{i}+\Delta\bar{i}}$ share an $(n-1, \ell+1)$ -intersection and thus, by Assumption 3, there exists a shortest chain between them. Moreover, from the definitions of A_i^j and B_i^j , there exist \mathbf{r}_0 and $\bar{\mathbf{r}}_1$ such that $\bar{\mathbf{i}} \in D_{\ell, \ell+1}^j(\mathbf{i} + \mathbf{r}_0)$ and $\bar{\mathbf{i}} + \Delta\bar{\mathbf{i}} \in D_{\ell, \ell+1}^j(\mathbf{i} + \bar{\mathbf{r}}_1 + (m_k + 1)\delta_k)$. Thus, the following inequalities hold *component-wise*,

$$\begin{aligned} \mathbf{j} - \mathbf{1} \leq \mathbf{i} + \mathbf{r}_0 - \bar{\mathbf{i}} \leq \mathbf{0}, \\ \mathbf{j} - \mathbf{1} \leq \mathbf{i} + \bar{\mathbf{r}}_1 + (m_k + 1)\delta_k - \bar{\mathbf{i}} - \Delta\bar{\mathbf{i}} \leq \mathbf{0}. \end{aligned}$$

In particular, the second inequality implies that

$$i_k + (m_k + 1) - \bar{i}_k \leq \Delta\bar{i}_k.$$

Next, since a shortest chain exists between $\alpha_{\bar{i}}$ and $\alpha_{\bar{i}+\Delta\bar{i}}$, let $\Delta\hat{\mathbf{i}}$ be such that it satisfies the following conditions:

- component-wise, $\mathbf{0} \leq \Delta\hat{\mathbf{i}} \leq \Delta\bar{\mathbf{i}}$;
- $\Delta\hat{i}_k = i_k + (m_k + 1) - \bar{i}_k \leq \Delta\bar{i}_k$;
- $\alpha_{\bar{i}+\Delta\hat{\mathbf{i}}} \in \mathcal{B}_{\ell, \ell+1}^0$ and $\text{supp}(\zeta) \subset \text{supp}(\phi) \subset \text{supp}(\alpha_{\bar{i}+\Delta\hat{\mathbf{i}}}) \subset B_i^j$.

Such a $\Delta\hat{\mathbf{i}}$ exists because of Assumption 3. In particular, the last condition implies that there exists $\bar{\mathbf{r}}_2$ such that

$$\mathbf{j} - \mathbf{1} \leq \mathbf{i} + \bar{\mathbf{r}}_2 + (m_k + 1)\delta_k - \bar{\mathbf{i}} - \Delta\hat{\mathbf{i}} \leq \mathbf{0},$$

with equality holding on the right for the k th component because of the definition of $\Delta\hat{i}_k$. Therefore, we see that the following inequality holds *component-wise*,

$$\mathbf{0} \leq \bar{\mathbf{i}} + \Delta\hat{\mathbf{i}} - \mathbf{i} - \bar{\mathbf{r}}_2 - (m_k + 1)\delta_k \leq \mathbf{1} - \mathbf{j} - \delta_k.$$

Therefore, $\bar{\mathbf{i}} + \Delta\hat{\mathbf{i}} \in D_{\ell, \ell+1}^{\mathbf{j}+\delta_k}(\mathbf{i} + \bar{\mathbf{r}}_2 + (m_k + 1)\delta_k)$ and consequently $\text{supp}(\alpha_{\bar{i}+\Delta\hat{\mathbf{i}}}) \subset B_i^{\mathbf{j}+\delta_k}$. This implies that

$$\mathcal{B}_{\ell+s, \ell+1}^*(A_i^j) \cap \mathcal{B}_{\ell+s, \ell+1}^*(B_i^j) \subset \mathcal{B}_{\ell+s, \ell+1}^*(B_i^{\mathbf{j}+\delta_k}) \subset \mathcal{B}_{\ell+s, \ell+1}^*(A_i^j \cap B_i^j).$$

Finally, from Lemma 4.11, if $\phi \in \mathcal{B}_{\ell+s, \ell+1}^*(A_i^j \cap B_i^j)$ then $\phi \in \mathcal{B}_{\ell+s, \ell+1}^*(A_i^j)$ and $\phi \in \mathcal{B}_{\ell+s, \ell+1}^*(B_i^j)$. As a result

$$\mathcal{B}_{\ell+s, \ell+1}^*(A_i^j \cap B_i^j) \subset \mathcal{B}_{\ell+s, \ell+1}^*(A_i^j) \cap \mathcal{B}_{\ell+s, \ell+1}^*(B_i^j).$$

The claim of equation (52) follows. □

Corollary 4.19 *With A_i^j and B_i^j defined as in Lemma 4.18,*

$$\mathcal{X}_{\ell+s}(\square) = \mathcal{X}_{\ell+s, \ell+1}(\square) \tag{53}$$

for $\square \in \{A_i^j, B_i^j, B_i^{j+\delta_k}, A_i^j \cap B_i^j\}$.

Proof For $\square \in \{A_i^j, B_i^j, B_i^{j+\delta_k}\}$, equation (53) follows directly from Lemma 4.13 and application of Assumption 3. It remains to show that $\mathcal{X}_{\ell+s}(A_i^j \cap B_i^j) = \mathcal{X}_{\ell+s, \ell+1}(A_i^j \cap B_i^j)$. By definition, $\mathcal{X}_{\ell+s}(A_i^j \cap B_i^j) \supset \mathcal{X}_{\ell+s, \ell+1}(A_i^j \cap B_i^j)$. The reverse inclusion holds since

$$\begin{aligned} f &\in \mathcal{X}_{\ell+s}(A_i^j \cap B_i^j), \\ \Rightarrow f &\in \mathcal{X}_{\ell+s}(A_i^j) \cap \mathcal{X}_{\ell+s}(B_i^j), \\ \Rightarrow f &\in \mathcal{X}_{\ell+s, \ell+1}(A_i^j) \cap \mathcal{X}_{\ell+s, \ell+1}(B_i^j), && \text{(Lemma 4.13)} \\ \Rightarrow f &\in \mathcal{X}_{\ell+s, \ell+1}(A_i^j \cap B_i^j) && \text{(Equation (52))}. \end{aligned}$$

□

Lemma 4.20 *For a fixed $1 \leq k \leq n$, let δ_k be an n -tuple with the value 1 in index k and 0 elsewhere, and let \mathbf{i}, \mathbf{j} and \mathbf{m} be given. Then, with $\bar{\mathbf{r}} := (r_1, \dots, r_{k-1}, 0, r_{k+1}, \dots, r_n)$ and with*

$$\begin{aligned} A_i^j &:= S_i^j[\mathbf{m}], \\ B_i^j &:= \bigcup_{r_1=0}^{m_1} \cdots \bigcup_{r_{k-1}=0}^{m_{k-1}} \bigcup_{r_{k+1}=0}^{m_{k+1}} \cdots \bigcup_{r_n=0}^{m_n} \Omega_{\ell+1}^j(\mathbf{i} + \bar{\mathbf{r}} + (m_k + 1)\delta_k), \\ C_i^j &:= S_i^j[\mathbf{m} + \delta_k], \end{aligned}$$

the following holds for $s = 0, 1$,

$$\mathcal{B}_{\ell+s, \ell+1}^*(A_i^j) \cup \mathcal{B}_{\ell+s, \ell+1}^*(B_i^j) = \mathcal{B}_{\ell+s, \ell+1}^*(A_i^j \cup B_i^j) = \mathcal{B}_{\ell+s, \ell+1}^*(C_i^j). \tag{54}$$

In the above a superscript of $*$ denotes that the statement is true for all B-splines, i.e., for all possible superscripts.

Proof From Lemma 4.17, $A_i^j \cup B_i^j = C_i^j$, and so we focus only on the first equality of the claim. However, the containment $\mathcal{B}_{\ell+s, \ell+1}^*(A_i^j) \cup \mathcal{B}_{\ell+s, \ell+1}^*(B_i^j) \subset \mathcal{B}_{\ell+s, \ell+1}^*(A_i^j \cup B_i^j)$ again follows from Lemma 4.11.

For the other direction, if $\phi \in \mathcal{B}_{\ell+s, \ell+1}^j(A_i^j \cup B_i^j)$, then by Assumption 3 and Lemma 4.13, there exists some $\alpha_0 \in \mathcal{B}_\ell^0(A_i^j \cup B_i^j) = \mathcal{B}_{\ell+\ell+1}^0(A_i^j \cup B_i^j)$ such that $\text{supp}(\phi) \subset \text{supp}(\alpha_0)$. But then $\text{supp}(\alpha_0) \subset A_i^j$ or $\text{supp}(\alpha_0) \subset B_i^j$ by construction. As a result, $\phi \in \mathcal{B}_{\ell+s, \ell+1}^j(A_i^j)$ or $\phi \in \mathcal{B}_{\ell+s, \ell+1}^j(B_i^j)$. \square

We are now ready to show how the above results and Eq. (49) can be used to show exactness of the hierarchical spline complex. We will do this by considering some special slices $S_i^j[\mathbf{m}]$. In the following, we fix $\mathbf{i} = (i_1, \dots, i_n)$, $\mathbf{j} = (j_1, \dots, j_n)$, and for $k \geq 1$ define

$$\mathbf{i}_k := \sum_{l=1}^k \delta_l + \sum_{l=k+1}^n i_l \delta_l, \quad \mathbf{j}_k := \sum_{l=k+1}^n j_l \delta_l, \tag{55a}$$

$$S[k, m_k] := \bigcup_{r_1=0}^{m(\ell,1)} \cdots \bigcup_{r_{k-1}=0}^{m(\ell,k-1)} \bigcup_{r_k=0}^{m_k} \Omega_{\ell+1}^{\mathbf{j}_k} \left(\mathbf{i}_k + \sum_{l=1}^k r_l \delta_l \right), \tag{55b}$$

$$S[k] := S[k, m(\ell, k)]. \tag{55c}$$

Observe that, from Eq. (49), $S[n] = \Omega_{\ell+1}$. Moreover, we will say that a domain, say B , is an $S[k]$ -type domains if it is defined as above but with possibly different choices of \mathbf{i} and \mathbf{j} .

Proposition 4.21 *Let Assumption 3 hold. Then, the inclusion operation*

$$\iota_{\ell, \ell+1} : \mathcal{X}_{\ell, \ell+1}(S[1]) \rightarrow \mathcal{X}_{\ell+1, \ell+1}(S[1]) \tag{56}$$

induces an isomorphism on the cohomology of the spline spaces.

Proof We will show the claim for $S[1]$ by considering $S[1, m_1]$ and inducting on m_1 . For the base case of $m_1 = 0$, the claim follows from Corollary 4.15. Assume that the claim is true for some $m_1 \geq 0$ and, as in Lemmas 4.18 and 4.20, define

$$A := S[1, m_1], \quad B := \Omega_{\ell+1}^{\mathbf{j}_1}(\mathbf{i}_1 + (m_1 + 1)\delta_1), \quad C := S[1, m_1 + 1].$$

Thus, the induction hypothesis is that the following map induces an isomorphism on the spline cohomology,

$$\iota_{\ell, \ell+1} : \mathcal{X}_{\ell, \ell+1}(A) \rightarrow \mathcal{X}_{\ell+1, \ell+1}(A),$$

and our objective is to show that the same is true for

$$\iota_{\ell, \ell+1} : \mathcal{X}_{\ell, \ell+1}(C) \rightarrow \mathcal{X}_{\ell+1, \ell+1}(C).$$

First, observe that Lemma 4.13 implies that $\mathcal{X}_{\ell+s,\ell+1}(\square) = \mathcal{X}_{\ell+s}(\square)$ for any $\square \in \{A, B, C\}$, and Corollary 4.19 implies $\mathcal{X}_{\ell+s,\ell+1}(A \cap B) = \mathcal{X}_{\ell+s}(A \cap B)$. Moreover, from Theorem 4.5, the following diagram commutes,

$$\begin{array}{ccccccc} \dots & \rightarrow & H_\ell^{(j)}(A \cap B) & \rightarrow & H_\ell^{(j)}(A) \oplus H_\ell^{(j)}(B) & \rightarrow & H_\ell^{(j)}(A \boxplus B) \rightarrow H_\ell^{(j+1)}(A \cap B) \rightarrow \dots \\ & & \downarrow & & \downarrow & & \downarrow & & \downarrow \\ \dots & \rightarrow & H_{\ell+1}^{(j)}(A \cap B) & \rightarrow & H_{\ell+1}^{(j)}(A) \oplus H_{\ell+1}^{(j)}(B) & \rightarrow & H_{\ell+1}^{(j)}(A \boxplus B) \rightarrow H_{\ell+1}^{(j+1)}(A \cap B) \rightarrow \dots \end{array}$$

Using Corollary 4.15 and Lemma 4.18, the first vertical map is an isomorphism for all j . By the inductive hypothesis and Corollary 4.15, the same is true for the second vertical map. Then, from Corollary 4.6, the third vertical map is also an isomorphism. This proves the claim since, from Lemma 4.20, the spline complex $\mathcal{X}_{\ell+s}(A \boxplus B)$ is the same as $\mathcal{X}_{\ell+s}(A \cup B) = \mathcal{X}_{\ell+s}(C)$ for $s = 0, 1$. \square

Proposition 4.22 *Let Assumption 3 hold. Then, the inclusion operation*

$$\iota_{\ell,\ell+1} : \mathcal{X}_{\ell,\ell+1}(S[n]) \rightarrow \mathcal{X}_{\ell+1,\ell+1}(S[n]) \tag{57}$$

induces an isomorphism on the cohomology of the spline spaces.

Proof We proceed by looking at $S[k]$ and inducting on k . The claim follows for the base case $k = 1$ from Proposition 4.21. Next, given $k \geq 1$, assume that the following inclusion induces an isomorphism on spline cohomology,

$$\iota_{\ell,\ell+1} : \mathcal{X}_{\ell,\ell+1}(S[k]) \rightarrow \mathcal{X}_{\ell+1,\ell+1}(S[k]) . \tag{\star}$$

Our objective is to show that the same is true for $k + 1$,

$$\iota_{\ell,\ell+1} : \mathcal{X}_{\ell,\ell+1}(S[k + 1]) \rightarrow \mathcal{X}_{\ell+1,\ell+1}(S[k + 1]) . \tag{*}$$

This will complete the proof and we proceed by inducting on subdomains of $S[k + 1]$.

Nested induction for $S[k + 1, m_{k+1}]$: We will show the claim for $S[k + 1]$ by considering $S[k + 1, m_{k+1}]$ and inducting on m_{k+1} . The base case of $m_{k+1} = 0$ follows from the induction hypothesis in (\star) since $S[k + 1, 0] = S[k]$. Assume that the claim is true for some $m_{k+1} \geq 0$ and, as in Lemma 4.18, define

$$\begin{aligned} A &:= S[k + 1, m_{k+1}], \quad C := S[k + 1, m_{k+1} + 1] \\ B_{\mathbf{i}_{k+1}}^{\mathbf{j}_{k+1}} &:= \bigcup_{r_1=0}^{m(\ell,1)} \dots \bigcup_{r_k=0}^{m(\ell,k)} \Omega_{\ell+1}^{\mathbf{j}_{k+1}} \left(\mathbf{i}_{k+1} + \sum_{l=1}^k r_l \delta_l + (m_{k+1} + 1) \delta_{k+1} \right) . \end{aligned}$$

Simple two-dimensional examples of such domains are shown in Fig. 5, while more involved three-dimensional examples are shown in Fig. 6. Thus, the induction hypothesis is that the following map induces an isomorphism on the spline cohomology,

$$\iota_{\ell,\ell+1} : \mathcal{X}_{\ell,\ell+1}(A) \rightarrow \mathcal{X}_{\ell+1,\ell+1}(A),$$

and our objective is to show that the same is true for

$$\iota_{\ell, \ell+1} : \mathcal{X}_{\ell, \ell+1}(C) \rightarrow \mathcal{X}_{\ell+1, \ell+1}(C).$$

First, note that $\mathcal{B}_{\ell+s, \ell+1}^*(A \cap B_{i_{k+1}}^{j_{k+1}}) = \mathcal{B}_{\ell+s, \ell+1}^*(B_{i_{k+1}}^{j_{k+1}+\delta_{k+1}})$ by Lemma 4.18. Since both $B_{i_{k+1}}^{j_{k+1}}$ and $B_{i_{k+1}}^{j_{k+1}+\delta_{k+1}}$ are domains of $S[k]$ -type domains, the following inclusion map induces an isomorphism on the spline cohomology from the induction hypothesis (\star),

$$\iota_{\ell, \ell+1} : \mathcal{X}_{\ell, \ell+1}(\square) \rightarrow \mathcal{X}_{\ell+1, \ell+1}(\square), \quad \square \in \left\{ B_{i_{k+1}}^{j_{k+1}}, B_{i_{k+1}}^{j_{k+1}+\delta_{k+1}} \right\}. \quad (\dagger)$$

Next, for any $\square \in \{A, B_{i_{k+1}}^{j_{k+1}}, C, A \cap B_{i_{k+1}}^{j_{k+1}}\}$, Lemma 4.13 and Corollary 4.19 imply that $\mathcal{X}_{\ell+s, \ell+1}(\square) = \mathcal{X}_{\ell+s}(\square)$, $s = 0, 1$. Then, following the same line of reasoning as in Proposition 4.21, Theorem 4.5 implies the following commuting diagram,

$$\begin{array}{ccccccc} \dots & \rightarrow & H_{\ell}^{(j)}(A \cap B_{i_{k+1}}^{j_{k+1}}) & \rightarrow & H_{\ell}^{(j)}(A) \oplus H_{\ell}^{(j)}(B_{i_{k+1}}^{j_{k+1}}) & \rightarrow & H_{\ell}^{(j)}(A \boxplus B_{i_{k+1}}^{j_{k+1}}) \rightarrow H_{\ell}^{(j+1)}(A \cap B_{i_{k+1}}^{j_{k+1}}) \rightarrow \dots \\ & & \downarrow & & \downarrow & & \downarrow \\ \dots & \rightarrow & H_{\ell+1}^{(j)}(A \cap B_{i_{k+1}}^{j_{k+1}}) & \rightarrow & H_{\ell+1}^{(j)}(A) \oplus H_{\ell+1}^{(j)}(B_{i_{k+1}}^{j_{k+1}}) & \rightarrow & H_{\ell+1}^{(j)}(A \boxplus B_{i_{k+1}}^{j_{k+1}}) \rightarrow H_{\ell+1}^{(j+1)}(A \cap B_{i_{k+1}}^{j_{k+1}}) \rightarrow \dots \end{array}$$

The first vertical map is an isomorphism for all j from (\dagger), and the second vertical map is an isomorphism for all j from the induction hypotheses on $A = S[k+1, m_{k+1}]$ and (\dagger). Therefore, so is the third vertical map from Corollary 4.6. Since, from Lemma 4.20, the spline complex $\mathcal{X}_{\ell+s}(A \boxplus B_{i_{k+1}}^{j_{k+1}}) = \mathcal{X}_{\ell+s}(A \cup B_{i_{k+1}}^{j_{k+1}}) = \mathcal{X}_{\ell+s}(C)$ for $s = 0, 1$, this completes the induction on m_{k+1} and, consequently, on k . \square

Theorem 4.23 *Let Assumption 3 hold. Then, the hierarchical chain complex*

$$0 \xrightarrow{c} \mathcal{W}_{\ell}^0 \xrightarrow{d} \mathcal{W}_{\ell}^1 \xrightarrow{d} \dots \xrightarrow{d} \mathcal{W}_{\ell}^n \xrightarrow{f} \mathbb{R} \rightarrow 0 \quad (58)$$

is exact for any $0 \leq \ell \leq L$.

Proof Since $S[n] = \Omega_{\ell+1}$ for $i = 1$, Theorem 5.5 of [12] states that the hierarchical B-spline complex is exact as the following inclusion induces isomorphisms on spline cohomology $\forall \ell$,

$$\iota_{\ell, \ell+1} : \mathcal{X}_{\ell, \ell+1}(\Omega_{\ell+1}) \rightarrow \mathcal{X}_{\ell+1, \ell+1}(\Omega_{\ell+1}).$$

\square

5 Implementation and Validation

A thorough investigation of the numerical stability of these spline spaces, as well as a discussion of practical implementation and refinement strategies, is outside of the scope of this paper. Instead, we discuss some basic ideas for computationally verifying that assumptions are satisfied for a particular refinement configuration and

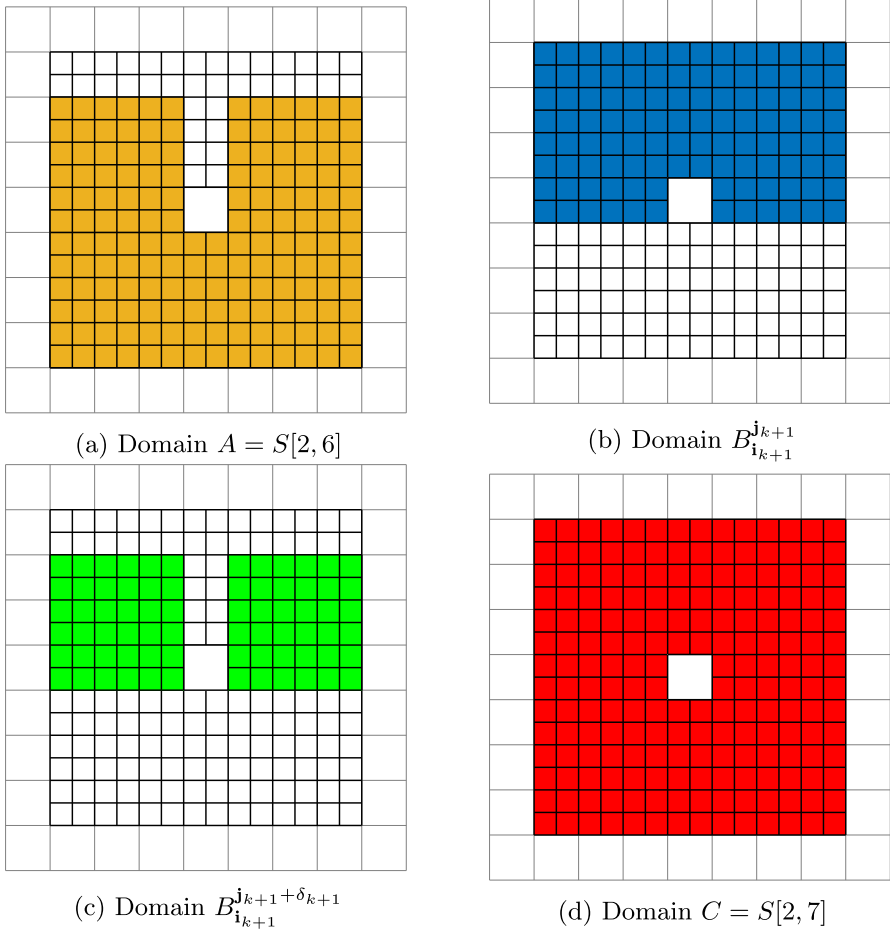


Fig. 5 The above figures correspond to a maximally regular hierarchical spline space defined using $p_{(\ell,k)} = 2$ for all ℓ and k . For $k = 1$, and with the proof of Proposition 4.22 as reference (the part on nested induction), example domains A , $B_{i_{k+1}}^{j_{k+1}}$, $B_{i_{k+1}}^{j_{k+1} + \delta_{k+1}}$ and C are shown for this hierarchical configuration for $m_{k+1} = 6$

then investigate the (in)exactness of various refinement configurations. Future work will explore numerical stability, approximation power of the spline spaces, and a-posteriori error analysis.

5.1 Verifying Assumption 3 for a Given Refinement Configuration

Given a hierarchical refinement configuration, it is clear from the formulation of Assumption 3 that its verification only requires information from pairs of successive refinement levels.

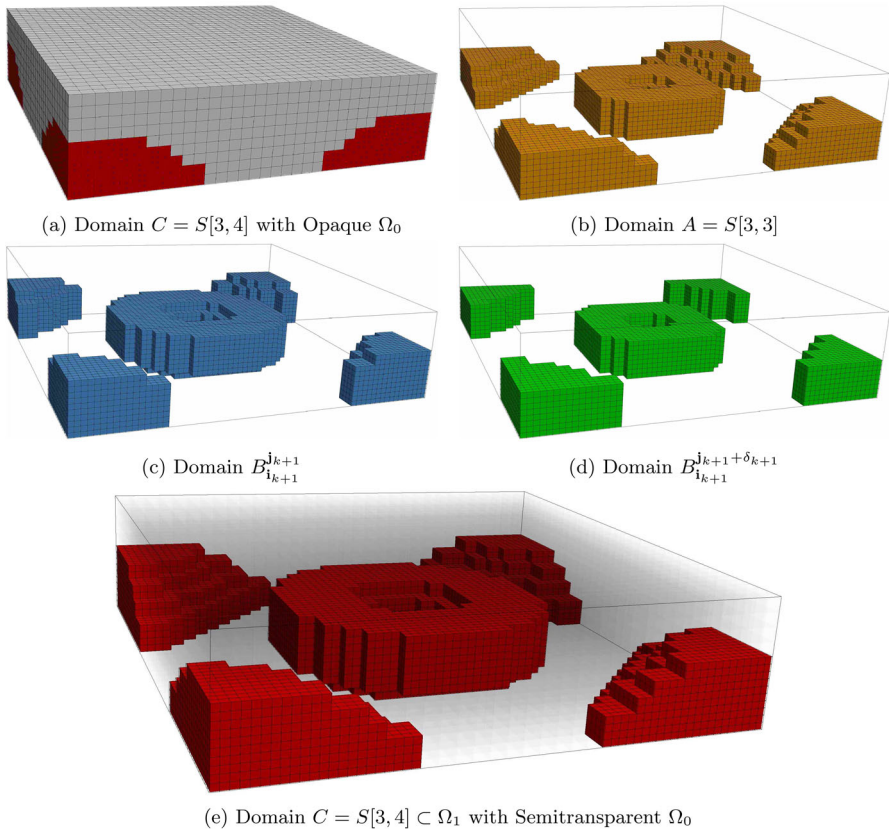


Fig. 6 The above figures correspond to a maximally regular hierarchical spline space defined using $p(\ell, k) = 3$ for all ℓ and k . For $k = 2$, and with the proof of Proposition 4.22 as reference (the part on nested induction), example domains A , $B_{i_{k+1}}^{j_{k+1}}$, $B_{i_{k+1}}^{j_{k+1} + \delta_{k+1}}$ and C are shown for this hierarchical configuration for $m_{k+1} = 3$

In this subsection, we explicitly state how Assumption 3 can be verified in a computer implementation.

Condition 1 Let $0 \leq \ell \leq L - 1$, \mathbf{i} be the index of a 0-form B-spline of level ℓ , and define $I_{\ell, \ell+1}^{k, -}$ and $I_{\ell, \ell+1}^{k, +}$ to be the following maps,

$$I_{\ell, \ell+1}^{k, -}(\mathbf{i}) := \min \{l : \xi_{l, \ell+1, k} = \xi_{i_k, \ell, k}\},$$

$$I_{\ell, \ell+1}^{k, +}(\mathbf{i}) := \max \{l : \xi_{l, \ell+1, k} = \xi_{i_k + p(\ell, k) + 1, \ell, k}\}.$$

Consider $\alpha_{\mathbf{i}}, \alpha_{\mathbf{i} + \Delta \mathbf{i}} \in \mathcal{B}_{\ell, \ell+1}^0$ and, without loss of generality, let $\Delta \mathbf{i}$ be component-wise non-negative. Then,

$\text{supp}(\alpha_i), \text{supp}(\alpha_{i+\Delta i})$ share an $(n-1, \ell+1)$ -intersection

\Leftrightarrow

$$\left(I_{\ell, \ell+1}^{k,+}(\mathbf{i}) \geq I_{\ell, \ell+1}^{k,-}(\mathbf{i} + \Delta \mathbf{i}) \quad \forall k \in \{1, \dots, n\} \right) \text{ and}$$

$$\left(I_{\ell, \ell+1}^{k,+}(\mathbf{i}) - I_{\ell, \ell+1}^{k,-}(\mathbf{i} + \Delta \mathbf{i}) \geq p_{(\ell+1, k)} \quad \forall k \in \mathcal{I} \subset \{1, \dots, n\}, |\mathcal{I}| \geq (n-1) \right)$$

This is how we can check whether these splines share an $(n-1, \ell+1)$ intersection, as in Assumption 3. If they do not, then there is no need to check the second condition and the assumption is satisfied. On the other hand, such an intersection exists, then we need to check that the shortest path condition holds. This can be done as follows.

Condition 2 Assume that $\text{supp}(\alpha_i)$ and $\text{supp}(\alpha_{i+\Delta i})$ share an $(n-1, \ell+1)$ -intersection. Then, a simple computation reveals that there are at most $\prod_{k=1}^n (\Delta i_k + 1)$ shortest paths between α_i and $\alpha_{i+\Delta i}$. Each such shortest path will consist of B-splines $\alpha_{i+\Delta \hat{i}}$ such that $0 \leq \Delta \hat{i}_k \leq \Delta i_k$ holds for all k . Moreover, we also have $\Delta i_k \leq p_{(\ell, k)}$ since $\text{supp}(\alpha_i) \cap \text{supp}(\alpha_{i+\Delta i})$ contains at least one Bézier cell, a conservative upper bound that ignores the effect of repeated knots. Therefore, a brute force check on these limited number of shortest paths can be performed to verify that the second condition from Assumption 3 holds. For instance, for a potential shortest path, each B-spline $\alpha_{i+\Delta \hat{i}}$ in it must be such that all Bézier cells in its support have been refined.

Finally, let $B(\mathbf{i}, \Delta \mathbf{i}) \subset \mathcal{B}_{\ell, \ell+1}^0$ be the set of B-splines that form a shortest path between α_i and $\alpha_{i+\Delta i}$; by convention we assume that $\alpha_i, \alpha_{i+\Delta i} \in B(\mathbf{i}, \Delta \mathbf{i})$. Then, the shortest-path check does not need to be performed again for any $\alpha_a, \alpha_b \in B(\mathbf{i}, \Delta \mathbf{i})$ since the shortest path relation is commutative (the shortest path from α_a to α_b is also the shortest path from α_b to α_a) and obeys the following recursion condition: if there is a shortest path from α_a to α_c containing α_b , a subset of this path is a shortest path between α_a and α_b and another subset is a shortest path between α_b and α_c . This further reduces the computational workload behind this verification task.

Remark 5.1 While the above explicit and conservative approaches may not be the most efficient ones, they are easy to understand and illustrate how the conditions in Assumption 3 can be verified in a local manner for any given hierarchical refinement configuration, with the basic process amounting to a sequence of counting operations.

5.2 Example Applications and Limitations of Theorem 4.23

To verify that the current theory holds computationally, we construct the hierarchical B-spline complex of discrete differential forms for a variety of refinement configurations using extensions of GeoPDEs [27]. The computations involve finding the nullity of the matrix corresponding to the mixed discretization of the j -form Hodge Laplacian for the de Rham complex [1, Chapter 4] (e.g., using a QR or singular value decomposition) for all j . Specifically, this matrix corresponds to the following weak problem: find

$(g, f) \in \mathcal{W}_L^{j-1} \times \mathcal{W}_L^j$ such that

$$\begin{aligned} (v, g) - (dv, f) &= 0, & v \in \mathcal{W}_L^{j-1}, \\ (w, dg) + (dw, df) &= 0, & w \in \mathcal{W}_L^j. \end{aligned}$$

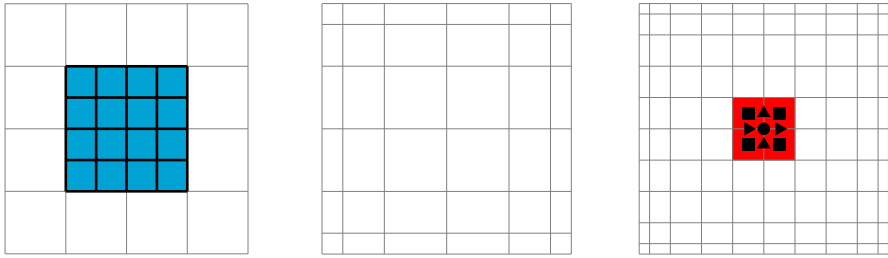
The hierarchical complex is exact in position j if the matrix corresponding to the above problem is of full rank for $j < n$ and has a nullity of one for $j = n$. Any increments in the nullity are in one-to-one correspondence with so-called discrete harmonic forms, i.e., spline functions in \mathcal{W}_L^j that are cocycles and are orthogonal to coboundaries. Existence of harmonic forms means the hierarchical spline complex is inexact, and the Hodge Laplacian is well-posed only up to these harmonic forms.

5.2.1 Inexact Refinement Configurations and Resulting Harmonics

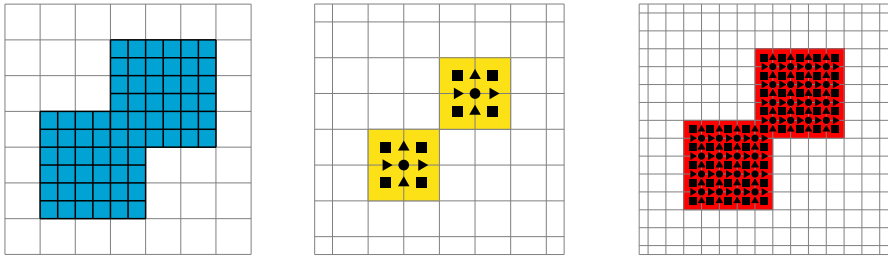
In this section, we build various hierarchical configurations that violate one or more assumptions leading up to Theorem 4.23. These are minimal examples for which spurious harmonic j -forms exist for $j > 0$. Spurious harmonic 0-forms cannot be created here because the imposition of homogeneous boundary conditions makes the 0-form Hodge Laplacian well-posed.

Two-dimensional examples In two dimensions, representative configurations that are inexact and their accompanying Greville meshes $\mathcal{G}_{0,1}$ and $\mathcal{G}_{1,1}$ (which manifest the change in the spline space topology) are shown in Fig. 7. The harmonic forms that are introduced as a result of this change in topology are shown in Fig. 8. In all cases, it can be seen that the homology of the Greville mesh changes between $\mathcal{G}_{0,1}$ and $\mathcal{G}_{1,1}$ to produce a spurious harmonic form. Introducing a new component (e.g. by violating Assumption 2) introduces additional harmonic 2-forms. Harmonic 1-forms are created by either merging two connected components of $\mathcal{G}_{0,1}$ into a single connected component in $\mathcal{G}_{1,1}$ or by modifying the topology of $\mathcal{G}_{0,1}$ from being a topological ball into a topological annulus on $\mathcal{G}_{1,1}$. In the case of Fig. 7 configuration (d), the refinement pattern introduces two harmonics because it transitions from refinement of two topological balls to a single connected component (introducing a harmonic 1-form) with non-trivial first homology group (introducing another harmonic 1-form).

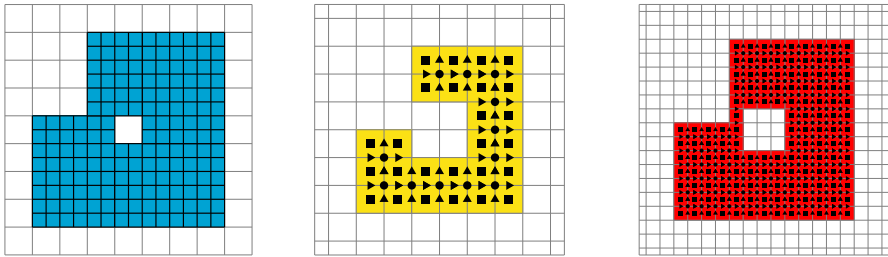
Three-dimensional examples Examples of refinement configurations resulting in spurious harmonics in three dimensions are depicted in Fig. 9. Similarly to two dimensions, each of these harmonics corresponds to a change in topology between $\mathcal{G}_{0,1}$ and $\mathcal{G}_{1,1}$. Specifically, harmonic 3-forms are introduced by violating Assumption 2 and including splines in the fine space that do not correspond to removal of splines in the coarse space. Harmonic 2-forms are introduced both by modifying $\mathcal{G}_{0,1}$ from a topological ball to a topological solid torus on $\mathcal{G}_{1,1}$ or by modifying $\mathcal{G}_{0,1}$ from being two topological balls into a single topological ball in $\mathcal{G}_{1,1}$. Similarly, harmonic 1-forms are produced by refinement patterns converting $\mathcal{G}_{0,1}$ from a topological ball into a configuration in $\mathcal{G}_{1,1}$ with an internal cavity or by refinement that converts $\mathcal{G}_{0,1}$ from being a solid torus into a topological ball in $\mathcal{G}_{1,1}$.



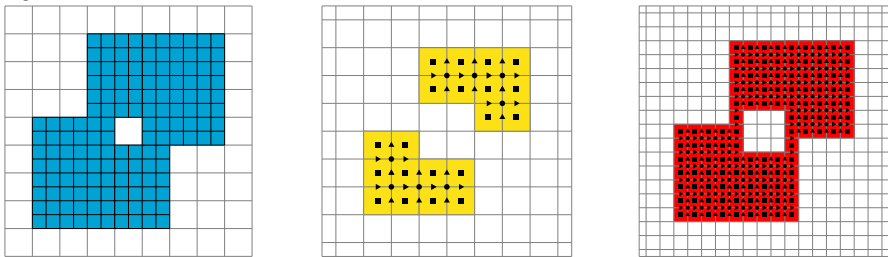
(a) Bicubic splines with maximal smoothness and Greville grid refinement from an empty domain to a topological ball.



(b) Biquadratic splines with maximal smoothness and refinement from two topological balls to a single topological ball



(c) Biquadratic splines with maximal smoothness and refinement from a topological ball to a topological annulus



(d) Biquadratic splines with maximal smoothness and refinement from two topological balls to a topological annulus

Fig. 7 Bézier meshes (left), coarse Greville subgrids $\mathcal{G}_{0,1}$ (center), and refined Greville subgrid $\mathcal{G}_{1,1}$ (right) for various inexact refinement schemes are shown. Inexactness can be visualized by the changes in the topology between $\mathcal{G}_{0,1}$ and $\mathcal{G}_{1,1}$ for the various configurations. Here, the filled disks correspond to Greville 0-cells, filled triangles correspond to Greville 1-cells, and filled squares correspond to Greville 2-cells

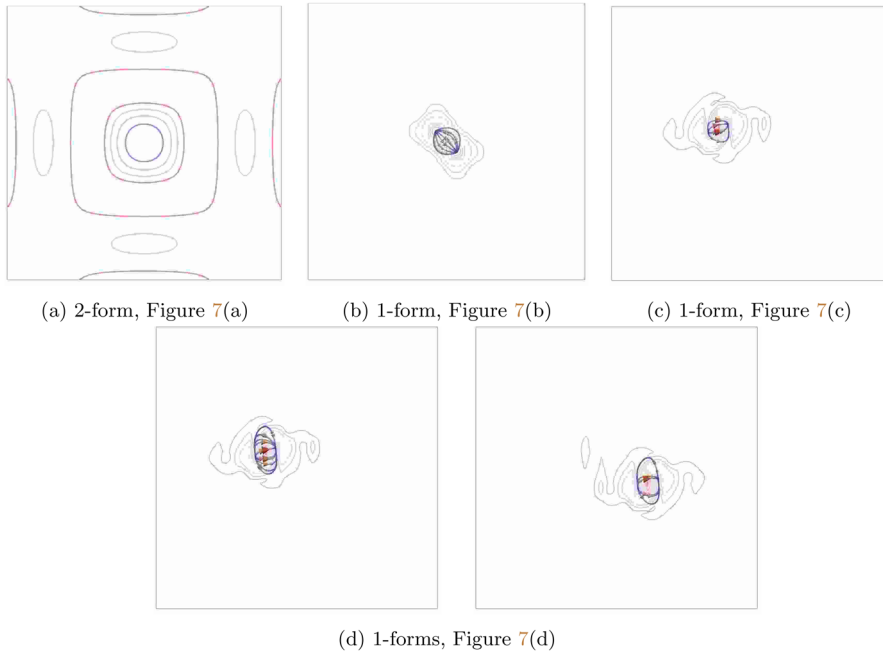


Fig. 8 Spurious harmonic forms introduced by refinement patterns of Fig. 7 are shown

5.2.2 Exact Refinement Patterns

Having characterized various harmonic forms and described minimal examples showing how changes in topology of the Greville meshes affect exactness of the hierarchical spline complex, we now turn our attention to certain configurations that lead to exact hierarchical spline complexes.

Two-dimensional examples In two dimensions, Fig. 10 shows a maximal regularity bi-degree (6, 6) hierarchical configuration where the refinement domain is built as the union of two 0-form B-splines; different subfigures correspond to different choices of the two B-splines. Table 4 compares these different configurations based on the local exactness characterization of [12] and our local exactness characterization presented herein. It can be seen that in some cases, the theory of [12] can capture refinements that violate at least one of our assumptions: this is because [12] permits refinement of 2-form B-splines rather than just 0-form B-splines (see Assumption 2). That said, Assumption 3 of this work can be much less restrictive than Assumption 5.7 of [12]—particularly for high-degree splines with high smoothness. In the example shown, our proposed assumptions admits five of the six hierarchical configurations that are exact, while [12] only allows for two of them. This is largely because our result only requires identical topology between the coarse and fine Greville grids, while that of [12] is based on the more restrictive assumption requiring identical topologies for both the Beziér meshes and Greville grids. On the other hand, the assumptions proposed in this

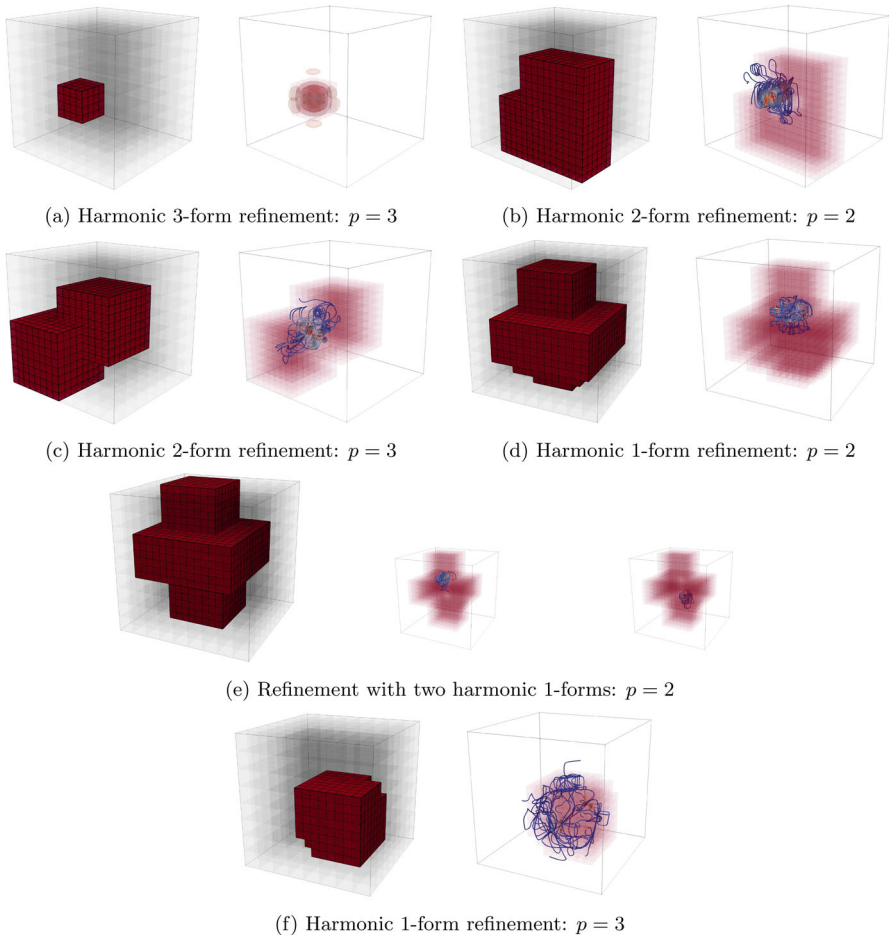


Fig. 9 Inexact refinement patterns in three dimensions are shown for trivariate splines of degree $p_{(\ell,k)} = p$ and maximal smoothness for all ℓ and k . Each refinement pattern leads to $\mathcal{G}_{0,1}$ to $\mathcal{G}_{1,1}$ with different topologies. Pattern (a) introduces a new component in $\mathcal{G}_{1,1}$, pattern (b) transitions from a ball topology in $\mathcal{G}_{0,1}$ to a solid torus in $\mathcal{G}_{1,1}$, pattern (c) transitions from two disconnected balls in $\mathcal{G}_{0,1}$ to one in $\mathcal{G}_{1,1}$, pattern (d) transitions from a ball in $\mathcal{G}_{0,1}$ to a simply connected volume with a void in $\mathcal{G}_{1,1}$, pattern (e) transitions from a solid torus in $\mathcal{G}_{0,1}$ to a simply connected volume with a void in $\mathcal{G}_{1,1}$, and pattern (f) transitions from a solid torus in $\mathcal{G}_{0,1}$ to a ball in $\mathcal{G}_{1,1}$.

work can also be restrictive in other situations as they require refinement along paths of 0-forms (see Definition 4.3).

Three-dimensional examples A variety of exact refinement patterns in three dimensions are depicted in Figs. 11 and 12. Figure 11 exhibits exact refinement patterns that are permitted by this work, while Fig. 12 shows exact refinements that are not permissible given our assumptions.

Since the local exactness condition of [12] does not apply for $n > 2$, we do not compare exact refinement patterns of this work to those of others. That said, in [12,

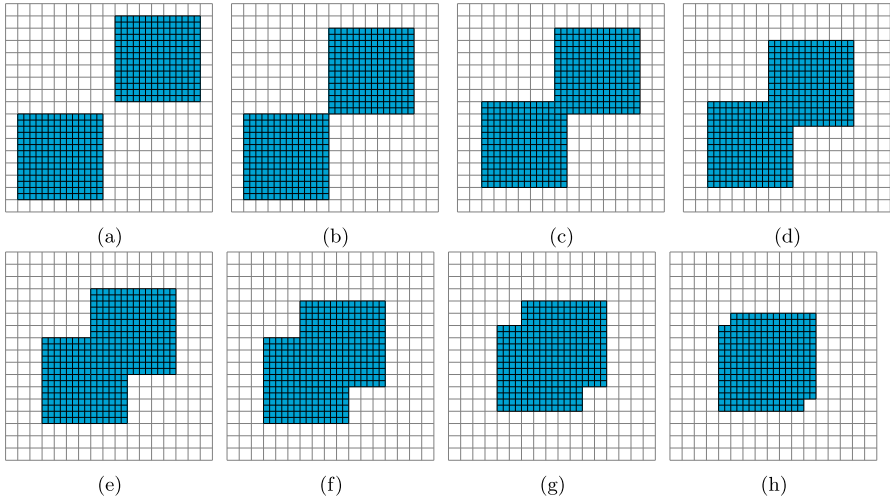


Fig. 10 The above figures show hierarchical meshes used for building maximally smooth hierarchical B-splines with $p_{(\ell,k)} = 6$ for all ℓ and k . The domain $\Omega_{\ell+1}$ is defined to be the union of the supports of two 0-form B-splines at level ℓ . Different subfigures correspond to different choices of the two B-splines and each subfigure progressively leads to a greater overlap of their respective supports. Refinement patterns (e–g) are not exact, while all others are. The assumptions given in this document allow for each of the exact refinement patterns except figure (h), while those of [12] are more restrictive in this respect and cannot capture three of them

Table 4 For the refinement patterns shown in Fig. 10, the table below presents whether the corresponding hierarchical complexes are exact, and whether the local exactness constraints of this work and those of [12] are met

Refinement pattern	Exact	Assumption 5.7 [12]	Assumption 3
Figure 10a	Yes	Yes	Yes
Figure 10b	Yes	No	Yes
Figure 10c	Yes	No	Yes
Figure 10d	Yes	No	Yes
Figure 10e	No	No	No
Figure 10f	No	No	No
Figure 10g	No	No	No
Figure 10h	Yes	Yes	No

Since refinements are performed by combining the supports of two 0-forms, Assumption 2 of this work and Assumption 5.6 of [12] are always satisfied and so we do not include them in the table

Remark 5.9] it is conjectured that the hierarchical B-spline complex would be exact if the intersection between the support of any j -form of Ω_ℓ and the complement of $\Omega_{\ell+1}$ is homologically trivial (i.e. the zeroth homology group has rank one and all others are of rank zero). This is a direct extension of [12, Assumption 5.7] to higher-dimensional spaces. The results of this paper do not contradict this claim. Nonetheless, our results show that this conjecture may be more restrictive than is necessary. Indeed, Assumption 3 does not require the topology of the coarse and fine Greville grids to match that of the underlying Beziér mesh, as the conjecture of [12] would. The

exact refinement patterns of Fig. 11 permissible under this work illustrate this point: refinements presented in subfigures (a)-(c) would be supported by the extension of [12] to three dimensions, while the refinement patterns in subfigures (d)-(k) would be inadmissible. We believe that in higher dimensions permissible refinement patterns under the conjecture of [12] would be similarly much too restrictive.

Finally, the results of this numerical study appear to indicate that our proposed refinement strategy on 0-forms may be more restrictive than a refinement pattern that simply relies on refinement of n -forms, as does [12]. We postulate that Assumptions 2 and 3 could be modified to only operate on n forms, rather than 0-forms, and still produce a sufficient local exactness result. Arriving at such a proof, however, would require more advanced techniques than available herein and, in particular, may preclude the use of the Mayer-Vietoris sequence. We expect that such a result, however, would both generalize and unify the theory of this work and that of [12].

6 Conclusions

The incorporation of smooth, locally-refinable splines within the framework of *finite element exterior calculus* can help build stable, accurate and efficient numerical methods. Motivated by this, we have presented a theoretical analysis of a discrete de Rham complex built using hierarchical B-splines on a hypercube $\Omega \subset \mathbb{R}^n$. In particular, we have presented locally-verifiable conditions that are sufficient for ensuring exactness of this discrete de Rham complex. These theoretical results are accompanied by numerical tests to showcase their applicability. These numerical tests help us investigate the different refinement patterns allowed by our assumptions and, in the special case of $n = 2$, allow us to contrast our approach with the one from [12]. We find that our approach is applicable to certain refinement patterns disallowed by [12] and vice versa. Future work should aim to unify the strengths of each approach. There are other promising lines of theoretical and applied research that can follow this manuscript, and in the following we briefly introduce some extensions of interest.

For applications, perhaps the most obvious case of interest is the use of our results for building stable adaptive numerical methods for problems in electromagnetism and fluid mechanics on domains in \mathbb{R}^3 . A first interesting open problem here is, given meshes that do not satisfy Assumption 3, how to transform them into meshes that do by adding minimal number of degrees of freedom. Another practical extension is the incorporation of boundary conditions other than Dirichlet boundary conditions. Alternatively, for solving problems on an arbitrary domain Ω , it will be interesting to build a discrete complex by performing a cuboidal decomposition of Ω and piecing together the discrete spline complexes defined on each cuboidal subdomain.

There are also several theoretical follow-ups that are of interest in numerical analysis. Since exactness of the discrete complex is only one of the ingredients in the construction of stable numerical methods, an interesting question is whether there exist commuting projection operators from the continuous complex to the exact discrete subcomplexes that we consider in this document. Similarly, constructive methods for building local commuting projection operators is of interest for both theoretical and applied studies.

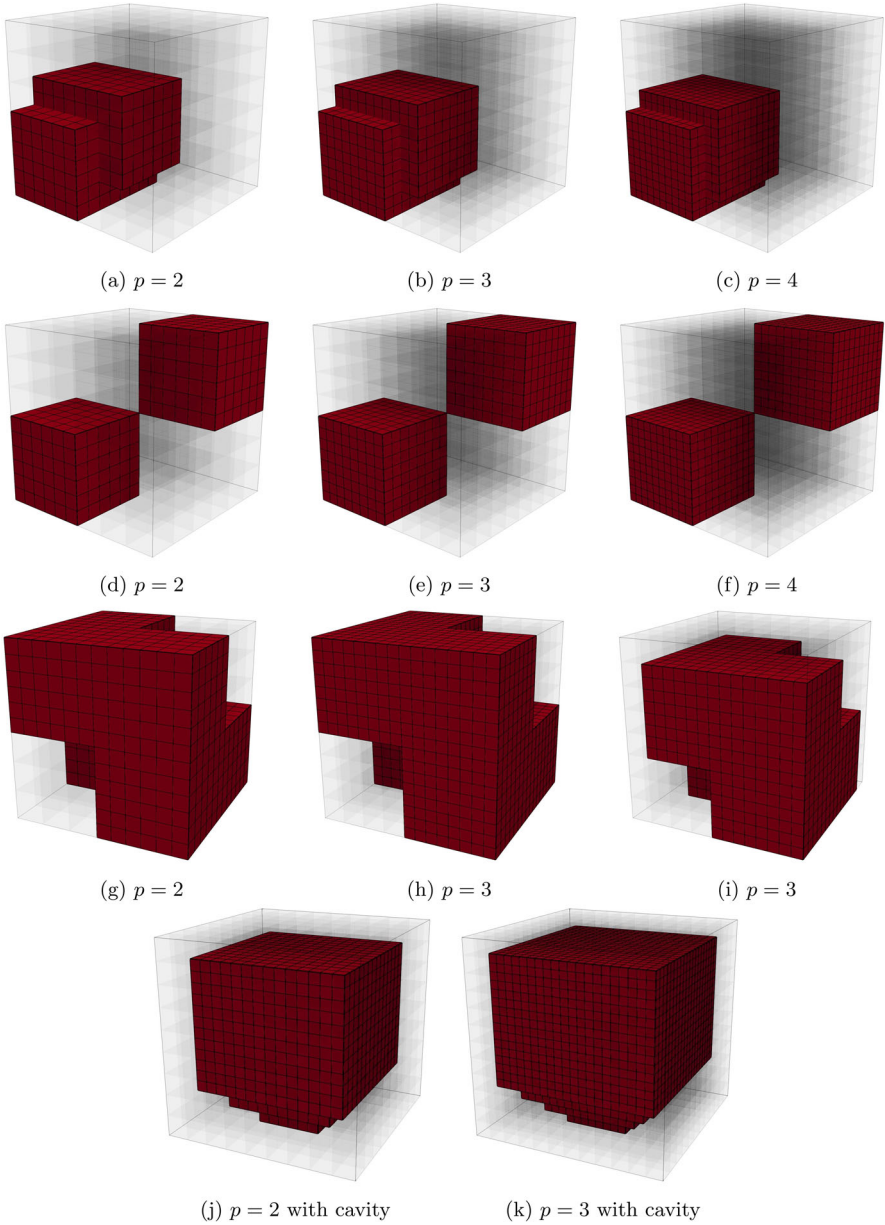


Fig. 11 Examples of refinement patterns for splines of maximal smoothness allowed by the proposed local exactness condition are shown above. The Greville grids $\mathcal{G}_{0,1}$ to $\mathcal{G}_{1,1}$ for the refinement patterns in each row are, respectively, a single contractible domain, two disconnected contractible domains, a single component with a non-trivial loop, and a single component with a void

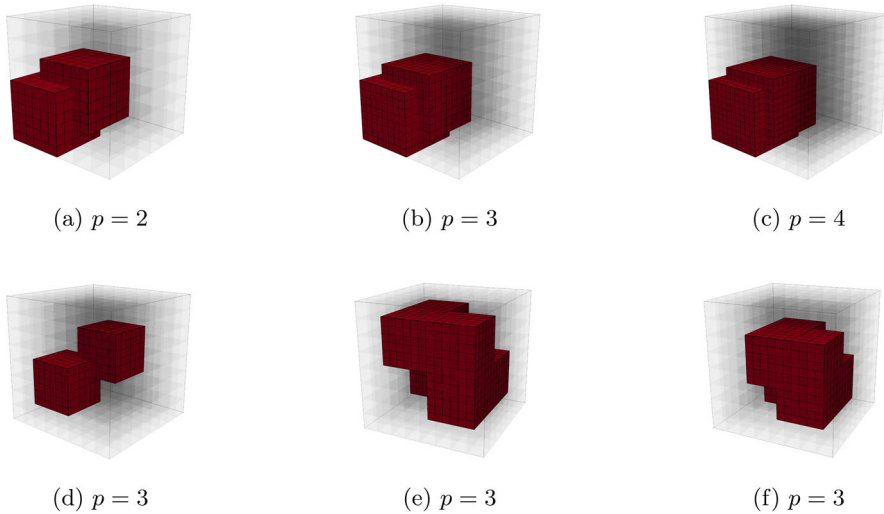


Fig. 12 Refinement patterns that are not supported based on the proposed local exactness condition, but that are exact, are shown above. In the first row, there is no shortest path of translation operators going between the two refined 0-form basis functions: to meet the proposed criteria, additional refinement would need to be made, e.g., as in the first row of Fig. 11. In the second row, refinements are made using the support of three-form basis functions, rather than 0-form basis functions

Acknowledgements K. Shepherd was partially supported by the National Science Foundation Graduate Research Fellowship under Grant No. DGE-1610403. Any opinion, findings, and conclusions or recommendations expressed in this material are those of the authors and do not necessarily reflect the views of the National Science Foundation. The research of Deepesh Toshniwal is supported by project number 212.150 awarded through the Veni research programme by the Dutch Research Council (NWO).

Open Access This article is licensed under a Creative Commons Attribution 4.0 International License, which permits use, sharing, adaptation, distribution and reproduction in any medium or format, as long as you give appropriate credit to the original author(s) and the source, provide a link to the Creative Commons licence, and indicate if changes were made. The images or other third party material in this article are included in the article's Creative Commons licence, unless indicated otherwise in a credit line to the material. If material is not included in the article's Creative Commons licence and your intended use is not permitted by statutory regulation or exceeds the permitted use, you will need to obtain permission directly from the copyright holder. To view a copy of this licence, visit <http://creativecommons.org/licenses/by/4.0/>.

References

1. D.N. Arnold. Finite Element Exterior Calculus. CBMS-NSF regional conference series in applied mathematics. *Society for Industrial and Applied Mathematics*, Philadelphia, PA, 2018.
2. D.N. Arnold, R.S. Falk, and R. Winther. Finite element exterior calculus, homological techniques, and applications. *Acta Numer.*, 15:1–155, 2006.
3. D.N. Arnold, R.S. Falk, and R. Winther. Finite element exterior calculus: from Hodge theory to numerical stability. *Bull. Amer. Math. Soc. (N.S.)*, 47(2):281–354, 2010.
4. Y. Bazilevs, M.-C. Hsu, and M.A. Scott. Isogeometric fluid–structure interaction analysis with emphasis on non-matching discretizations, and with application to wind turbines. *Comput. Methods Appl. Mech. Engrg.*, 249:28–41, 2012.

5. Andrea Bressan and Espen Sande. Approximation in FEM, DG and IGA: a theoretical comparison. *Numerische Mathematik*, 143(4):923–942, 2019.
6. A. Buffa, J. Rivas, G. Sangalli, and R. Vázquez. Isogeometric discrete differential forms in three dimensions. *SIAM J. Numer. Anal.*, 49(2):818–844, 2011.
7. A. Buffa, G. Sangalli, and R. Vázquez. Isogeometric analysis in electromagnetics: B-splines approximation. *Comput. Methods Appl. Mech. Engrg.*, 199(17-20):1143 – 1152, 2010.
8. A. Buffa, G. Sangalli, and R. Vázquez. Isogeometric methods for computational electromagnetics: B-spline and T-spline discretizations. *J. Comput. Phys.*, 257, Part B:1291–1320, 2014.
9. C. de Boor. *A Practical Guide to Splines*, volume 27 of *Applied Mathematical Sciences*. Springer-Verlag, New York, revised edition, 2001.
10. J.A. Evans, Y. Bazilevs, I. Babuška, and T.J.R. Hughes. N-widths, sup-infs, and optimality ratios for the k -version of the isogeometric finite element method. *Comput. Methods Appl. Mech. Engrg.*, 198:1726–1741, 2009.
11. J.A. Evans and T.J.R. Hughes. Isogeometric divergence-conforming B-splines for the Darcy-Stokes-Brinkman equations. *Math. Models Methods Appl. Sci.*, 23(04):671–741, 2013.
12. J.A. Evans, M.A. Scott, K.M. Shepherd, D.C. Thomas, and R. Vázquez. Hierarchical B-spline complexes of discrete differential forms. *IMA J. Numer. Anal.*, 39:preprint, 2019.
13. G. Farin. *Curves and surfaces for CAD: a practical guide*. Morgan Kaufmann, 2002.
14. D. Ferus. Analysis III: Wintersemester 2007/8, 2008. Course lecture notes.
15. A. Hatcher. *Algebraic topology*. Cambridge University Press, Cambridge, 2002.
16. T.J.R. Hughes, J.A. Cottrell, and Y. Bazilevs. Isogeometric analysis: CAD, finite elements, NURBS, exact geometry and mesh refinement. *Comput. Methods Appl. Mech. Engrg.*, 194(39-41):4135–4195, 2005.
17. T.J.R. Hughes. *The finite element method*. Prentice Hall Inc., Englewood Cliffs, NJ, 1987.
18. K.A. Johannessen, M. Kumar, and T. Kvamsdal. Divergence-conforming discretization for Stokes problem on locally refined meshes using LR B-splines. *Comput. Methods in Appl. Mech. Engrg.*, 293:38–70, 2015.
19. D. Kamensky, M.-C. Hsu, Y. Yu, J.A. Evans, M.S. Sacks, and T.J.R. Hughes. Immersogeometric cardiovascular fluid-structure interaction analysis with divergence-conforming B-splines. *Comput. Methods in Appl. Mech. Engrg.*, 314:408–472, 2017.
20. R. Krafft. Adaptive and linearly independent multilevel B-splines. In *Surface Fitting and Multiresolution Methods (Chamonix–Mont-Blanc, 1996)*, pages 209–218. Vanderbilt Univ. Press, Nashville, TN, 1997.
21. B. Perse, K. Kormann, and E. Sonnendrücker. Geometric particle-in-cell simulations of the Vlasov–Maxwell system in curvilinear coordinates. *SIAM Journal on Scientific Computing*, 43(1):B194–B218, 2021.
22. E. Sande, C. Manni, and H. Speleers. Sharp error estimates for spline approximation: Explicit constants, n -widths, and eigenfunction convergence. *Mathematical Models and Methods in Applied Sciences*, 29(06):1175–1205, 2019.
23. L. Schumaker. *Spline functions: basic theory*. Cambridge University Press, 2007.
24. M. Spivak. *Calculus on Manifolds*. Addison-Wesley, New York, NY, 1995.
25. M. Spivak. *A Comprehensive Introduction to Differential Geometry*, volume 1. Publish or Perish, Inc., Houston, TX, 3 edition, 1999.
26. D. Toshniwal and T.J.R. Hughes. Isogeometric discrete differential forms: Non-uniform degrees, bézier extraction, polar splines and flows on surfaces. *Computer Methods in Applied Mechanics and Engineering*, 376:113576, 2021.
27. R. Vázquez. A new design for the implementation of isogeometric analysis in Octave and Matlab: GeoPDEs 3.0. *Comput. Math. Appl.*, 72(3):523–554, 2016.
28. A.-V. Vuong, C. Giannelli, B. Jüttler, and B. Simeon. A hierarchical approach to adaptive local refinement in isogeometric analysis. *Comput. Methods Appl. Mech. Engrg.*, 200(49-52):3554–3567, 2011.